protocol (Invitrogen). First-strand cDNA was synthesized from 1 μg total RNA using SuperscriptIII reverse transcriptase (Invitrogen) and a random or oligo-dT primer. Semi-quantitative PCR was done essentially as described [Okuda et al., 2006]. Primers used for RT-PCR analysis of mRNA expression in zebrafish extracts were as follows: for *mkk4a*, 5′-CGTTC AACAG TAGAC GAGCG-3′ and 5′-AATCA CTTCG TCTAA AGAGG-3′; for *mkk4b*, 5′-CGCTC CACGG TGGAT GAGAA-3′ and 5′-AATGA CGTCA TCTGA CGCAC-3′; for *mkk7*, 5′-TGGCC ATGTC ATCGC AGTCA-3′ and 5′-GGAAA CTGTC CTGTG GCTAG-3′; for *β-actin*, 5′-CAGCT TCACC ACCAC AGC-3′ and 5′-GTGGA TACCG CAAGA TTCC-3′; for *jnk1a-1*, 5′-AGCGT ATGAC CACGT CCTCG-3′ and 5′-GGGCC AGACC GAAAT CCAG-3′; for *jnk1a-2*, 5′-GGATG CTTAC ACATC GACTT CAC-3′ and 5′-CATCC ATCAG CTCCA TTACT AGG-3′; for *jnk2*, 5′-ATCTG GACCA TGAGA GGATG TC-3′ and 5′-CTGGG GTTTG TTCAT CACAT AG-3′; for *e-cadherin*, 5′-ACAAA CTTAG GGCTC ATGCG-3′ and 5′-ACAGA TGCAG TGTAC GAGGA-3′; for *stat3*, 5′-TGAAT GGAAA CAGCC AGGCA-3′ and 5′-TTTGA TGACA AGGGG TCGGT-3′; for *liv1*, 5′-CGGTT GCCAA TATGA TTGGC-3′ and 5′-GGTGG ATTCC TGGTT CATCT-3′; for *wnt5*, 5′-CCGGA GATGT ACATC ATTGG-3′ and 5′-TTCTC ACGTT CACGA GCGTC-3′; for *wnt11*, 5′-GTAAA CTTCT GGACG GGCTC-3′ and 5′-CGAAG GTTAT CTCCA CATCC-3′.

ZEBRAFISH EMBRYO PREPARATION

Embryos were deyolked with deyolking buffer (1/2 Ginzburg Fish Ringer) without calcium [Link et al., 2006]. Subsequently embryos were lysed in buffer containing 100 mM NaCl, 40 mM Tris–HCl (pH 8.0), 1% Nonidet P-40, 0.05% 2-mercaptoethanol, 1 mM EDTA, 1 mM EGTA, 4 μg/ml aprotinin, 100 μM Na_3VO_4, and 50 mM NaF, and sonicated for 1 min. Lysates were centrifuged at 20,000*g* to pellet cellular debris. Protein concentration was measured by BCA™ Protein Assay Kit (Pierce).

ES CELL LINES

Mkk4$^{-/-}$ and *mkk7*$^{-/-}$ murine ES cell lines were generated as previously described [Nishina et al., 1997; Fleming et al., 2000; Kishimoto et al., 2003].

ANTIBODIES

Anti-Jnk1 polyclonal Ab (FL), which recognizes both the 46 and 55 kDa splice variants of Jnk1, was from Santa Cruz Biotechnology, Inc. Anti-phospho-Jnk (9251) and anti-FLAG (M2) Abs were from Cell Signaling Technology and Sigma–Aldrich Co., respectively.

CONSTRUCTION OF PLASMIDS AND TRANSFECTION

cDNAs encoding FLAG-tagged zebrafish Mkk4a-l, Mkk4b, and Mkk7 were cloned into the mammalian expression vector pCE-IRES2-EGFP [Ura et al., 2007]. ES cells were plated at 1×10^6 cells/35-mm dish and transfected 1 day later with expression construct (4 μg) plus Lipofectamine 2000 reagent (Invitrogen). Transfected cells were stimulated with UV light (1 kJ/m^2) and subjected to standard Western blot analysis as described below.

WESTERN BLOT ANALYSIS

Proteins were fractionated by SDS–PAGE and transferred to a polyvinylidene difluoride membrane that was then incubated for 1 h in blocking solution (2% or 5% skim milk in Tris-buffered saline [TBS]). The blocked membrane was incubated for 1 h in blocking solution containing anti-phospho-Jnk, anti-Jnk1, or anti-FLAG Ab. The membrane was then washed in TBS–Tween 20 (0.05%), incubated with anti-mouse/rabbit horseradish peroxidase-conjugated Ab (Jackson ImmunoResearch Laboratory) for 30 min, and washed three times in TBS–Tween 20. Proteins were visualized using Immobilon HRP (Millipore) or the SuperSignal West Femto Kit (Pierce) and a ChemiDoc XRS system (Bio-Rad), as described [Kishimoto et al., 2003].

ANTI-SENSE MORPHOLINO (MO) AND MRNA INJECTIONS

All MOs were designed to bind to exon–intron junctions and were synthesized by Gene Tools (Philomath, OR). Sequences of splice-blocking MOs were as follows: *mkk4a* MO, 5′-GATGA AACAG ACGAA CCTCT CTGAA-3′; *mkk4b* MO, 5′-TGTGT GTGTC TGACC TCTCT GAAGA-3′; *mkk7* MO, 5′-AGAGG AACTC ACCAG AGAAA TGCCA-3′; *jnk1a-1* MO, 5′-AGACA AATAA CTTAC ACATC CTGGA-3′; *jnk1a-2* MO, 5′-ATTTC AGTGT CTTGA CTTAC ATTTT-3′; *jnk2* MO, 5′-AAAAA CAGCA TTACC ATTCT CCTTG-3′. Sequences of translation-blocking MOs were: *mkk4a-l* atgMO, 5′-GCGTC GCCAT TTGGG TTTGA CTCTT-3′; *mkk4b* atgMO, 5′-AGAGT CACTG CTGGG AGCCG CCATT-3′; *mkk7* atgMO, 5′-AGAGT CTCTG CTCCA GCGAC GACAT-3′; *mkk4a-s* atgMO, 5′-GCCAT CTTGT TGACC GAGCC ATACG-3′. The standard control MO was: 5′-CCTCT TACCT CAGTT ACAAT TTATA-3′.

For knockdown, MO solution was injected into the yolks of one- to four-cell stage zebrafish embryos immediately beneath the cell body. For *wnt5* or *wnt11* overexpression, a construct designed to produce mRNA encoding full-length zebrafish *wnt5* or *wnt11* was created by cloning the relevant fragment (amplified by high-fidelity PCR) into the pCS2+ plasmid. A constitutively active form of Mkk4b (caMkk4b) was constructed by replacing Ser275 and Thr279 with aspartic acid and glutamic acid, respectively, and subcloning into the pCS2+ plasmid. Sense strand capped mRNA was synthesized using SP6 RNA polymerase and the mMESSAGE mMACHINE system (Ambion). RNA injections were performed as described [Shinya et al., 2000].

WHOLE-MOUNT IN SITU HYBRIDIZATION

Digoxigenin-labeled RNA probes were synthesized using the DIG RNA Labeling Kit (Roche Diagnostics). Primers used for mRNA expression analysis in whole zebrafish embryos were as follows: for *dlx3*, 5′-TCCGA CTTCT AAGGA CTCTC-3′ and 5′-TTCAC CTGTG TCTGT GTGAG-3′; for *ntl*, 5′-AGACG AATGT TTCCC GTGCT-3′ and 5′-CTTCT CTCTT TGGCA TCGAG-3′; for *hgg1*, 5′-ATGAG GAGTT CAGAC AGGCA-3′ and 5′-ATTAC CGCTG GGAAT GTCCA-3′; for *pax2.1*, 5′-CCGGC AGTAT TAAAC CTGGA-3′ and 5′-AGGTG CTTCC GTAAA CTCTC-3′; for *gsc*, 5′-GTCAC TATGA AGGAC ACTCG TGC-3′ and 5′-TTTGT TCCTG TTTTC AGGCG AC-3′; for *wnt5*, 5′-GTAGC AGACG TGAGC ACTGG-3′ and 5′-CGCAT TCCGA AAGTT CTTAA GAG-3′. Mixtures of three riboprobe pairs were used to detect *wnt11*, as follows: (1) 5′-GTAAA CTTCT GGACG GGCTC-3′ and 5′-CTAAA GTCCT GTGGG CCTGA-3′; (2) 5′-CCGGA ATTCA TGACA GAATA CAGGA ACT-3′ and 5′-CGAAG GTTAT CTCCA CATCC-3′; (3) 5′-GGTGC TTATG GACTC TCTAG-3′ and 5′-GAGTC GACTC

ACTTC GAGAC GTATC TCT-3′. Riboprobes for *myoD* and *krox20* were used as described [Shinya et al., 2000]. Whole mount in situ hybridization procedures were performed essentially as described [Thisse et al., 1993].

QUANTITATIVE REAL-TIME RT-PCR

Quantitative real-time RT-PCR analyses were performed using the Chromo4 real-time detection system (Bio-Rad). The PCR primers used were as follows: for *wnt11*, 5′-CACAA CAATG CTGTT GGCAG ACAGG TG-3′ and 5′-GGAGA TGGTG CTGAT GTCTT GAAGA CC-3′; for *β-actin*, 5′-GCAGA TGTGG ATCAG CAAGC AGG-3′ and 5′-CTGAG TCAAT GCGCC ATACA GAG-3′. For a 20 μl PCR reaction, cDNA template was mixed with 10 μl iQ SYBR Green Supermix (Bio-Rad) plus the appropriate primers to a final concentration of 200 nM each. The reaction was first incubated at 95°C for 3.5 min, followed by 41 cycles of 95°C for 12 s, 60°C for 13 s, and 72°C for 18 s.

RESULTS

CLONING AND CHARACTERIZATION OF ZEBRAFISH MKK4A, MKK4B, AND MKK7 GENES

To unravel the role of Jnk signaling in early zebrafish development, we first determined whether zebrafish *mkk4* and *mkk7* could function as direct activators of Jnk. We performed BLAST searches with mouse *mkk4* and *mkk7* to enable predictions of zebrafish *mkk4* and *mkk7* cDNA sequences. The obtained EST sequences were subjected to 5′- and 3′-RACE methodology to acquire the full-length cDNA sequences. The zebrafish has two *mkk4* genes, named *mkk4a* and *mkk4b* (GenBank accession no. AB438979), but only one *mkk7* ortholog (GenBank accession no. AB438980). The predicted amino acid (aa) sequences of the proteins encoded by these zebrafish genes are 81–84% identical to those of the mouse, and the Mkk phosphorylation sites are conserved (Fig. S1A). Two splice variants of zebrafish *mkk4a* were identified: *mkk4a-s* and *mkk4a-l* (GenBank accession nos. AB030901 and AB438978). Mkk4a-s (281 aa) is an N-terminal truncated form of Mkk4a-l (404 aa). A phylogenetic analysis of vertebrate *mkk4* genes revealed that zebrafish *mkk4a* was clustered with mammalian *mkk4* genes, whereas zebrafish *mkk4b* was clustered with those of other teleosts (Fig. S1B). These phylogenetic relationships suggest that the duplication of the *mkk4* gene occurred in the common ancestors of teleosts and tetrapods.

We next used semi-quantitative RT-PCR to examine the expression dynamics of *mkk4a*, *mkk4b*, and *mkk7* during early zebrafish development. All three genes were continuously expressed from the one-cell stage to the blastula (4.7 hpf) (Fig. 1A). Levels of both *mkk4a* and *mkk7* were markedly decreased by the shield stage and became relatively low at the tailbud stage. In contrast, *mkk4b* expression was essentially constant from the one-cell stage through to the shield stage and relatively high during later gastrula stages.

To monitor Jnk activity during zebrafish embryogenesis, we prepared protein extracts from zebrafish embryos collected at each of the 30% epiboly, shield, 75% epiboly, and tailbud stages, and examined the relative amounts of the active, phosphorylated form of Jnk by Western blot analysis. Jnk activity was detected from 30% epiboly and relatively high during later gastrula stages (Fig. 1B), suggesting the possibility that Jnk plays a role in the gastrulation stage.

In mammals, Mkk4 and Mkk7 have distinct biochemical properties and preferentially phosphorylate the Tyr and Thr residues, respectively, within the Thr-Pro-Tyr motif of Jnk [Lawler et al., 1998; Kishimoto et al., 2003]. To qualitatively determine whether these distinctions applied to the zebrafish orthologs of Mkk4 and Mkk7, and to gauge the functional relatedness of the mammalian and zebrafish enzymes, we analyzed whether zebrafish Mkks could compensate for the lack of mouse Mkk4 and Mkk7 in $mkk4^{-/-}$ and $mkk7^{-/-}$ murine ES cells, respectively. We transfected zebrafish *mkk4a-l*, *mkk4b*, and *mkk7* expression vectors separately into $mkk4^{-/-}$ or $mkk7^{-/-}$ ES cells, which lack the capacity to activate Jnk in response to UV irradiation [Nishitai et al., 2004]. We then subjected the transfected cells to UV irradiation and assessed Jnk activation. We found that zebrafish Mkk4a-l or Mkk4b, but not Mkk7, rescued UV-induced Jnk activation in $mkk4^{-/-}$ ES cells (Fig. 1C, lanes 2–4). Conversely, zebrafish Mkk7, but not Mkk4a-l or Mkk4b, rescued UV-induced Jnk activation in $mkk7^{-/-}$ ES cells (Fig. 1C, lanes 6–8). These results suggest that zebrafish Mkk4 and Mkk7 are analogous in function to their murine counterparts and play distinct biochemical roles during stress-induced Jnk activation.

ZEBRAFISH *MKK4B* IS INDISPENSABLE FOR NORMAL CE REGULATION

To elucidate the physiological roles of Mkk4a, Mkk4b, and Mkk7 during early zebrafish development, we performed anti-sense morpholino (MO)-mediated knockdown of each gene's mRNA and analyzed its residual expression by RT-PCR. Microinjection of *mkk4b* MO effectively prevented correct splicing of target pre-mRNA from the shield to tailbud stages (Fig. 2A). As a result, *mkk4b* morphants exhibited severe defects in anterior–posterior extension after gastrulation. At 11 hpf, *mkk4b* morphants displayed an MO dose-dependent shortening of body length (Fig. 2B, row 1) that did not recover at later developmental stages (Fig. 2B, rows 2 and 4). In addition, *mkk4b* morphants displayed broader notochords and somites during early segmentation than did control MO-injected embryos (Fig. 2B, row 3), indicating that CE is defective in the absence of Mkk4b. Quantification of the anterior–posterior axis extension and mediolateral convergence at 16 hpf revealed that *mkk4b* knockdown significantly increased the angle between the anterior and posterior ends of the embryo, as well as its mediolateral distance, in a MO dose-dependent manner (Fig. 2C).

With respect to marker expression patterns, *mkk4b* morphants showed a more posteriorly and broadly positioned prechordal plate (*hgg1*), a wider neural plate (*dlx3* and *pax2.1*), and a shorter and broader notochord (*ntl*) at the tailbud stage than did controls (Fig. 2D). Although their body axis was shorter and their somites wider, *mkk4b* morphants had the same numbers and shapes of rhombomeres (marked by *krox20* expression) and somites (*myoD*) as control embryos at the eight-somite stage (Fig. 2E), implying that Mkk4b has no obvious role in specifying cell fate.

To further confirm that it was loss of Mkk4b that was responsible for the observed CE defects, we co-injected *mkk4b*

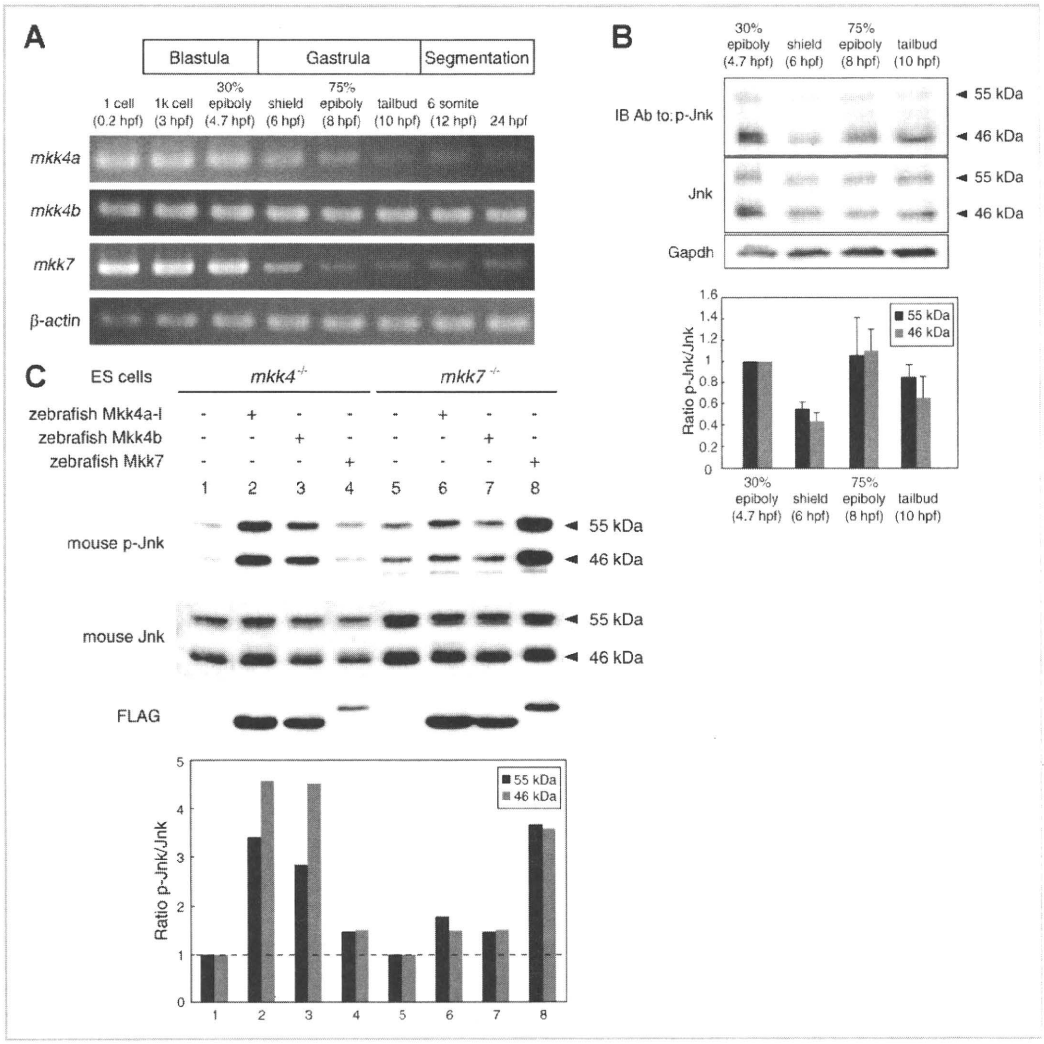

Fig. 1. Expression and biochemical properties of zebrafish *mkk4a*, *mkk4b*, and *mkk7* gene products during early development. A: Temporal expression patterns of zebrafish *mkks*. Semi-quantitative RT-PCR reveals relatively high expression of *mkk4b* up to 24 hpf in WT embryos, whereas *mkk4a* and *mkk7* levels abruptly decrease around the shield stage. Lanes 1–8 correspond to template cDNA derived from 0.2 to 24 hpf embryos (n = 30, 30, 50, 20, 20, 20, 30, 50 embryos, respectively). *β-Actin*, loading control. B: Analysis of Jnk activity during zebrafish embryogenesis. Approximately 50 μg of protein was loaded in SDS–PAGE in each lane. Activated Jnk and total Jnk were detected with anti-phospho-Jnk (p-Jnk) and anti-total-Jnk antibodies, respectively. Image shown is representative of three separate experiments with similar results (top). Graphic results are expressed as a ratio of p-Jnk to total Jnk and the value of 30% epiboly stage is assigned an arbitrary value of 1 (bottom). Data shown are the mean ± SEM of three independent experiments. C: Effects of zebrafish Mkk4 or Mkk7 expression on stress-induced Jnk activation in *mkk4*$^{-/-}$ or *mkk7*$^{-/-}$ mouse ES cells. *Mkk4*$^{-/-}$ or *mkk7*$^{-/-}$ mouse ES cells were transfected with zebrafish *mkk4a-l*, *mkk4b*, or *mkk7* expression vectors, cultured for 24 h, and stimulated with UV (1 kJ/m^2). Expression levels of zebrafish Mkks (FLAG) and endogenous levels of p-Jnk and total Jnk (46 and 55 kDa isoforms) in cell lysates were detected by Western blotting (top). The histogram shows quantitative representations of the relative activated Jnk, which was expressed as a ratio of p-Jnk to total Jnk (bottom). The values of lanes 1 and 5 are assigned an arbitrary value of 1.

MO with in vitro-transcribed *mkk4b* mRNA and assayed for the rescue of the CE defects. Inspection of live co-injected embryos showed that the synthetic *mkk4b* mRNA was able to prevent *mkk4b* MO-induced defects (Fig. S2). Thus, the observed phenotypes are the result of specific knockdown of Mkk4b by the *mkk4b* MO.

To rule out the possibility that the observed phenotypes in *mkk4b* knockdown embryos were secondary to a patterning alteration, we evaluated the distribution of *goosecoid* (*gsc*), a dorsal mesoderm "organizer" marker at the shield stage. No alterations to the *gsc* expression pattern were observed in *mkk4b* morphants (Fig. 2F), indicating that dorsoventral specification is not disturbed by *mkk4b* MO treatment.

The data in Figure 2D suggested that *mkk4b* morphants developed slightly slower than controls. To determine if Mkk4b influences epiboly, we monitored the development of live embryos over a time course of 6–10 hpf. As was true for control embryos, gastrulation began at 6 hpf in *mkk4b* morphants and 75% epiboly was reached at 8 hpf (Fig. S3). However, whereas control embryos had completed their epiboly movements by 10 hpf, *mkk4b* morphants exhibited a mild delay in epiboly that extended it to 11 hpf (Figs. S3 and 2B). Thus, Mkk4b activity is not required for the initiation or progression of epiboly but does influence its late phase.

When parallel experiments were used to examine the importance of Mkk4a in early zebrafish development, a very different result was

obtained. Microinjection of 0.8 pmol of *mkk4a* MO reduced WT *mkk4a* mRNA beginning at the shield stage (Fig. S4A). Unlike *mkk4b* morphants, however, *mkk4a* morphants had no gross morphological abnormalities (Fig. S4B), and the expression patterns of *hgg1*, *dlx3*, *ntl*, and *pax2.1* were completely normal (Fig. S4C).

In morphants injected with 0.8 pmol of *mkk7* MO, expression of the WT *mkk7* transcript declined by the shield stage and was undetectable at the tailbud stage (Fig. 2G). Instead, a shorter amplification product was detected. Like *mkk4b* morphants, *mkk7* morphants exhibited an MO dose-dependent shortening of body length at 24 hpf (Fig. 2H). However, the expression patterns of *hgg1*, *dlx3*, *ntl*, and *pax2.1* were normal in *mkk7* morphants, even at a high dose of MO (1.5 pmol) (Fig. 2I). These data suggest that *mkk7* is dispensable for proper gastrulation. Nevertheless, during

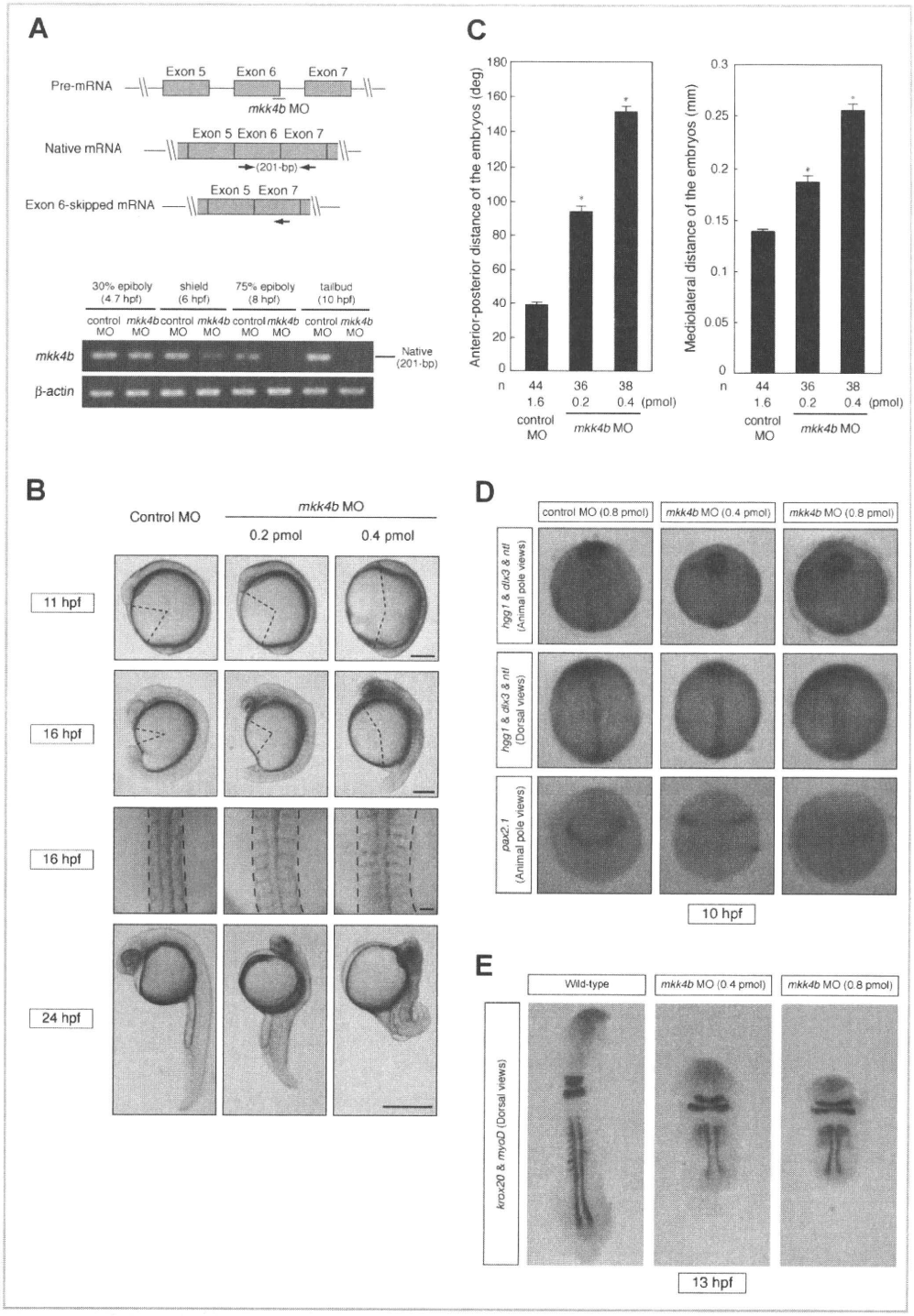

segmentation, the *mkk7* morphants displayed somites of abnormal patterning and morphology (Fig. 2J). Thus, Mkk7 function is essential for normal somite morphogenesis.

Because the *mkk4a*, *mkk4b*, and *mkk7* genes are maternally expressed, it was possible that their expression products might persist throughout gastrulation. To rule out this possibility, we used translation-blocking MOs (atgMOs) that would specifically target maternal and zygotic *mkk* transcripts and prevent their translation. We injected embryos with a specific translation-blocking MO (*mkk4a-l* atgMO, *mkk4b* atgMO, or *mkk7* atgMO) and examined their development using gross morphological analysis and in situ hybridization. By 23 hpf, *mkk4b* atgMO- or *mkk7* atgMO-injected embryos showed reduced body length compared to control-injected embryos, whereas few or no morphological differences were apparent in *mkk4a* atgMO-injected embryos (Fig. S5A). *Mkk4b* atgMO-injected embryos also showed altered expression of several marker genes (*hgg1*, *dlx3*, *ntl*, and *pax2.1*; Fig. S5B), highlighting the morphological abnormalities associated with defective CE movements at 10 hpf. This phenotype was strikingly similar to that of embryos subjected to *mkk4b* splice-blocking MO knockdown (Fig. 2D). Taken together, these results demonstrate that Mkk4b but not Mkk4a is essential for co-ordinated CE. In the following analyses, we focused on the specific role of Mkk4b–Jnk signaling in proper CE movements during gastrulation.

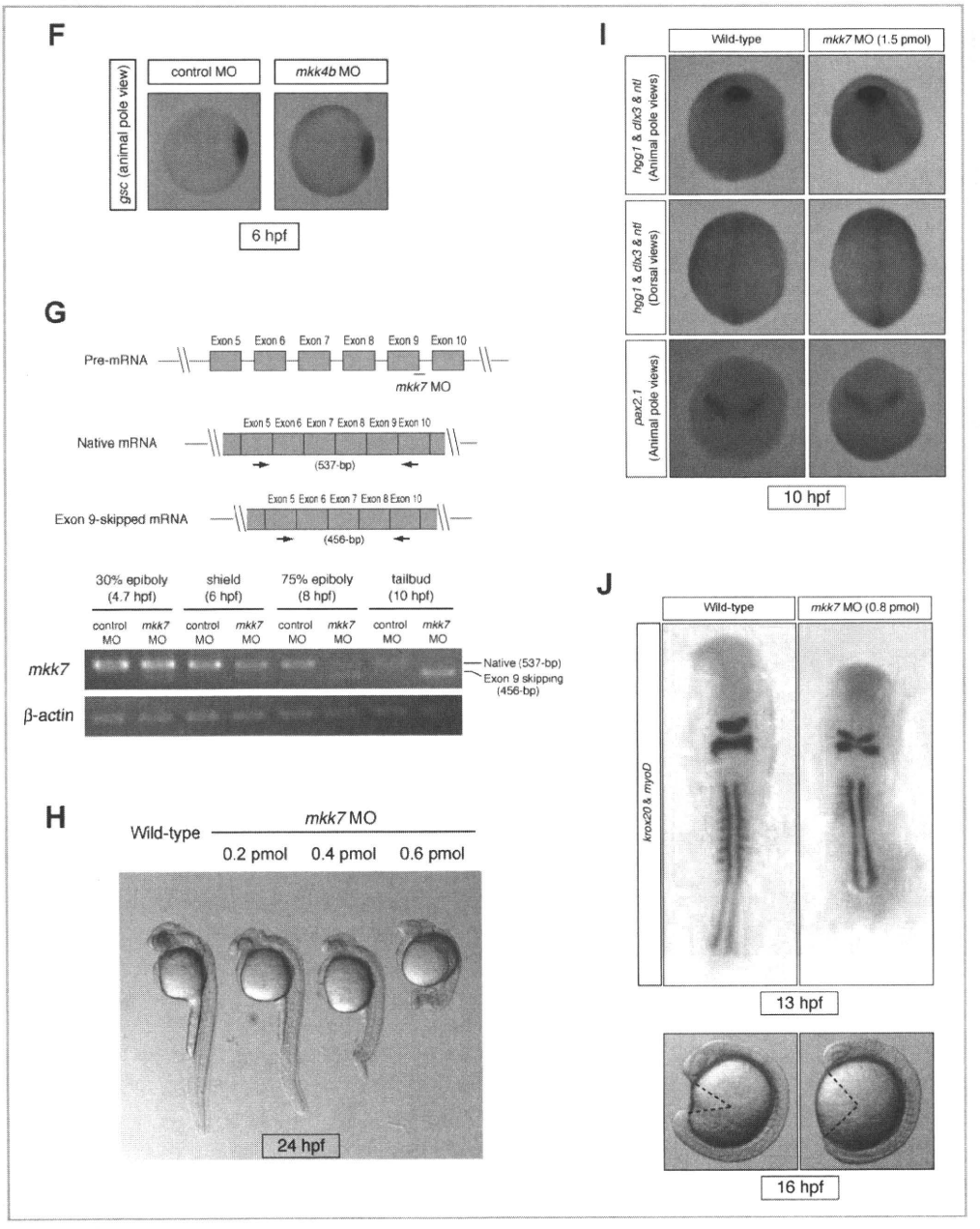

ZEBRAFISH JNK2 IS NECESSARY FOR CORRECT CE MOVEMENTS

It has previously been reported that non-canonical Wnt signaling regulates CE movements in *Xenopus* through the activation of Jnk [Yamanaka et al., 2002]. We therefore asked whether overexpression of *wnt11* or *wnt5* could activate Jnk during zebrafish gastrulation. Extracts from zebrafish embryos overexpressing *wnt11* or *wnt5* mRNA were prepared at 75% epiboly (8 hpf) and subjected to Western blotting with anti-phospho-Jnk antibody. This analysis confirmed that *wnt11* or *wnt5* overexpression significantly increased levels of the active, phosphorylated form of Jnk (Fig. 3A). Furthermore, analysis of extracts from embryos injected with 0.4 pmol *mkk4a* MO, *mkk4b* MO, or *mkk7* MO showed that Jnk phosphorylation was significantly decreased in *mkk4b* morphants but still detected in *mkk4a* and *mkk7* morphants (Fig. 3B). These data indicate that Mkk4b (exclusively) has a profound effect on CE, and that this effect is mediated through activation of the Jnk pathway. Thus, Mkk4b–Jnk signaling plays a critical role in proper CE movements during gastrulation.

To examine Mkk4b-Jnk signaling in zebrafish embryos, it was first necessary to identify zebrafish Jnk enzymes. To isolate zebrafish *jnk* genes, we used cDNA sequences for mammalian Jnks to perform BLAST searches of the zebrafish genomic database and identified four zebrafish *jnk* genes. A phylogenetic analysis based on the aa sequences of vertebrate Jnks revealed that the four zebrafish Jnk homologs closely resembled members of the three mammalian Jnk subfamilies, Jnk1, Jnk2, and Jnk3. We therefore designated the zebrafish proteins as Jnk1a-1, Jnk1a-2, Jnk2, and Jnk3 (Fig. S6). During gastrulation, mRNAs for Jnk1a-1, Jnk1a-2, and Jnk2 (but not Jnk3) were transcribed (data not shown).

To ascertain the functional importance of these zebrafish Jnk(s) for normal CE movements, we performed MO-mediated knockdown of the *jnk1a-1*, *jnk1a-2*, and *jnk2* genes and analyzed residual expression by RT-PCR. Co-injection of *jnk1a-1* MO and *jnk1a-2* MO efficiently prevented the correct splicing of *jnk1* pre-mRNAs during gastrulation (Fig. 3C). However, unlike the *Xenopus* Jnk1 morphant [Yamanaka et al., 2002], *jnk1a-1* and *jnk1a-2* morphants showed no gross morphological abnormalities (Fig. 3E, center), and the expression patterns of *hgg1*, *dlx3*, *ntl*, and *pax2.1* were completely normal (Fig. 3F, center). On the other hand, injection of *jnk2* MO not only prevented correct splicing of *jnk2* pre-mRNA (Fig. 3D) but also induced severe defects in anterior–posterior extension and mediolateral convergence, as assessed by analysis of morphology and molecular markers (Fig. 3E,F, right). These results indicate that Jnk2, but no form of Jnk1, is required for normal CE movements during zebrafish gastrulation.

TRANSCRIPTION OF ZEBRAFISH *WNT11* IS REPRESSED BY *MKK4B–JNK* SIGNALING

The molecular mechanism by which Jnk regulates CE movements is poorly understood. To identify relevant transcriptional targets downstream of the Mkk4b–Jnk signaling cascade associated with zebrafish CE, we used RT-PCR to survey mRNA levels of candidate genes in control and Mkk4b morphants at 75% epiboly (8 hpf). Because normal gastrulation requires modulation of cadherin-mediated cell–cell adhesion, we first investigated *e-cadherin* expression but found that its mRNA levels were unchanged in our morphants (Fig. 4A, row 1). Similarly, although *stat3* and *liv1* are reportedly essential for zebrafish gastrulation [Yamashita et al., 2004], the expression of these mRNAs was also normal in our *mkk* morphants (Fig. 4A, rows 2 and 3). We next screened components of the non-canonical Wnt pathway and found that, although *wnt5* expression was normal (Fig. 4A, row 4), *wnt11* expression was highly upregulated in Mkk4b-depleted embryos at 75% epiboly (8 hpf) (Fig. 4A, row 5), as well as at the 30% epiboly, shield, and tailbud stages (Fig. 4B, left). In contrast, upregulation of *wnt11* expression was not detected in Mkk4a- or Mkk7-depleted embryos (Fig. 4A). When we analyzed the expression of *wnt11* transcripts using quantitative real-time RT-PCR, we confirmed that levels

Fig. 2. Mkk4b–Jnk signaling is required for proper CE movements. A: Validation of *mkk4b* MO efficacy. The *mkk4b* MO targets the exon 6/intron 6 junction of *mkk4b* pre-mRNA as shown in the diagram (top). WT zebrafish embryos were injected with 0.8 pmol of *mkk4b* MO or control MO, and total RNA was extracted from the 30% epiboly to tailbud stages and subjected to RT-PCR analysis (bottom). Arrows in the diagram represent the primer pairs used for the RT-PCR analysis. The *mkk4b* MO efficiently prevents correct splicing of *mkk4b* pre-mRNA beginning at the shield stage (6 hpf), conceivably leading to a functional impairment of Mkk4b. B: Gross appearance of *mkk4b* MO-injected embryos. Images of a live control MO-injected embryo and live *mkk4b* morphants injected with the indicated doses of *mkk4b* MO were acquired at 11, 16, and 24 hpf (rows 1, 2, and 4, respectively). These embryos are viewed laterally, with anterior to the top. *Mkk4b* morphants exhibit a shortening of body length and brain degeneration in a MO dose-dependent manner. Row 3 shows that the notochord and somites are wider in the *mkk4b* morphant than in the control at 16 hpf (dorsal view). Scale bars = 200 μm (row 1); 200 μm (row 2); 50 μm (row 3); 500 μm (row 4). C: Quantification of anterior–posterior axis extension and mediolateral convergence at 16 hpf. Left panel shows the average angle between the anterior and posterior ends of embryos ($n = 44, 36, 38$) that were injected as indicated. Right panel shows the average mediolateral width of embryos ($n = 44, 36, 38$) that were injected as indicated. Data shown are the mean ± SEM. $^*P < 0.01$ versus control. D: Impaired CE in *mkk4b* morphants. Control MO-injected embryos and *mkk4b* morphants were analyzed by whole-mount in situ hybridization for the expression of tissue-specific genes at the tailbud stage (10 hpf). The position of the prechordal plate (*hgg1*) is more posterior and broader in *mkk4b* morphants compared to the control. Expression of *dlx3* (neuroectoderm) reveals a broader neural plate, and the notochord (*ntl*) is shorter and broader. The midbrain/hindbrain boundary (*pax2.1*) has expanded laterally. E: Normal rhombomeres in *mkk4b* morphants. WT embryos and *mkk4b* morphants had the same number and shape of rhombomeres (*krox20*) and somites (*myoD*) at the eight-somite stage (13 hpf), although the body axis was shorter and somites were wider in the *mkk4b* morphants. F: Expression of the dorsoventral patterning marker gene *gsc* is normal in *mkk4b* morphants. Control MO (0.8 pmol) or *mkk4b* MO (0.8 pmol) was injected into 1- to 4-cell embryos, which were analyzed by whole-mount in situ hybridization at the shield stage. Shown are animal pole views with dorsal to the right. For B and D–F, results shown are one experiment representative of at least three trials. G: Validation of *mkk7* MO efficacy as for A. Top: The *mkk7* MO targets the exon 9/intron 9 junction of *mkk7* pre-mRNA as shown in the diagram. Arrows represent primer pairs used in RT-PCR analysis. Bottom: The *mkk7* MO (0.8 pmol) causes a marked reduction in *mkk7* expression beginning at the shield stage (6 hpf). H: Gross appearance of *mkk7* MO-injected embryos. Images of a live untreated WT embryo and *mkk7* morphants injected with the indicated doses of *mkk7* MO were acquired at 24 hpf. All embryos are viewed laterally, with anterior to the top. *Mkk7* morphants exhibit weak, MO dose-dependent defects in the morphogenesis of the somites and a slightly shortened body length. I: Normal CE in *mkk7* morphants. WT embryos and *mkk7* morphants were analyzed for tissue-specific gene expression as for D. Even at a high dose of *mkk7* MO (1.5 pmol), the expression patterns of all tissue-specific genes examined were normal. J: Impaired somitogenesis in *mkk7* morphants. Top: The morphologies of rhombomeres (*krox20*) and somites (*myoD*) were examined at the eight-somite stage (13 hpf) in WT embryos and *mkk7* morphants. The body axis was shorter and the somites were wider in the latter (dorsal view). Bottom: Images of a live WT embryo (left) and live *mkk7* morphant (right) were acquired at 16 hpf (lateral view).

of *wnt11* mRNA were increased in *mkk4b* morphants (Fig. 4C). On the other hand, Mkk4b knockdown did not affect *wnt5* expression at any stage (Fig. 4B, right). These data indicate that Wnt11 itself is one of the molecular components downstream of the Jnk cascade in the non-canonical Wnt pathway associated with early embryogenesis.

We next examined whether activation of the Mkk4b–Jnk signaling pathway was sufficient to repress *wnt11* expression. Overexpression of a constitutively active form of Mkk4b (caMkk4b) markedly reduced the level of *wnt11* expression at 50% epiboly (Fig. 4D), reinforcing the notion that *wnt11* is a transcriptional target downstream of the Mkk4b–Jnk signaling cascade.

OVEREXPRESSION OF *WNT11* INDUCES ABNORMAL CE MOVEMENTS

To ascertain whether the increased *wnt11* expression in *mkk4b* morphants induced CE defects, we injected WT embryos with *wnt11* mRNA. Embryos overexpressing *wnt11* mRNA showed a shortening

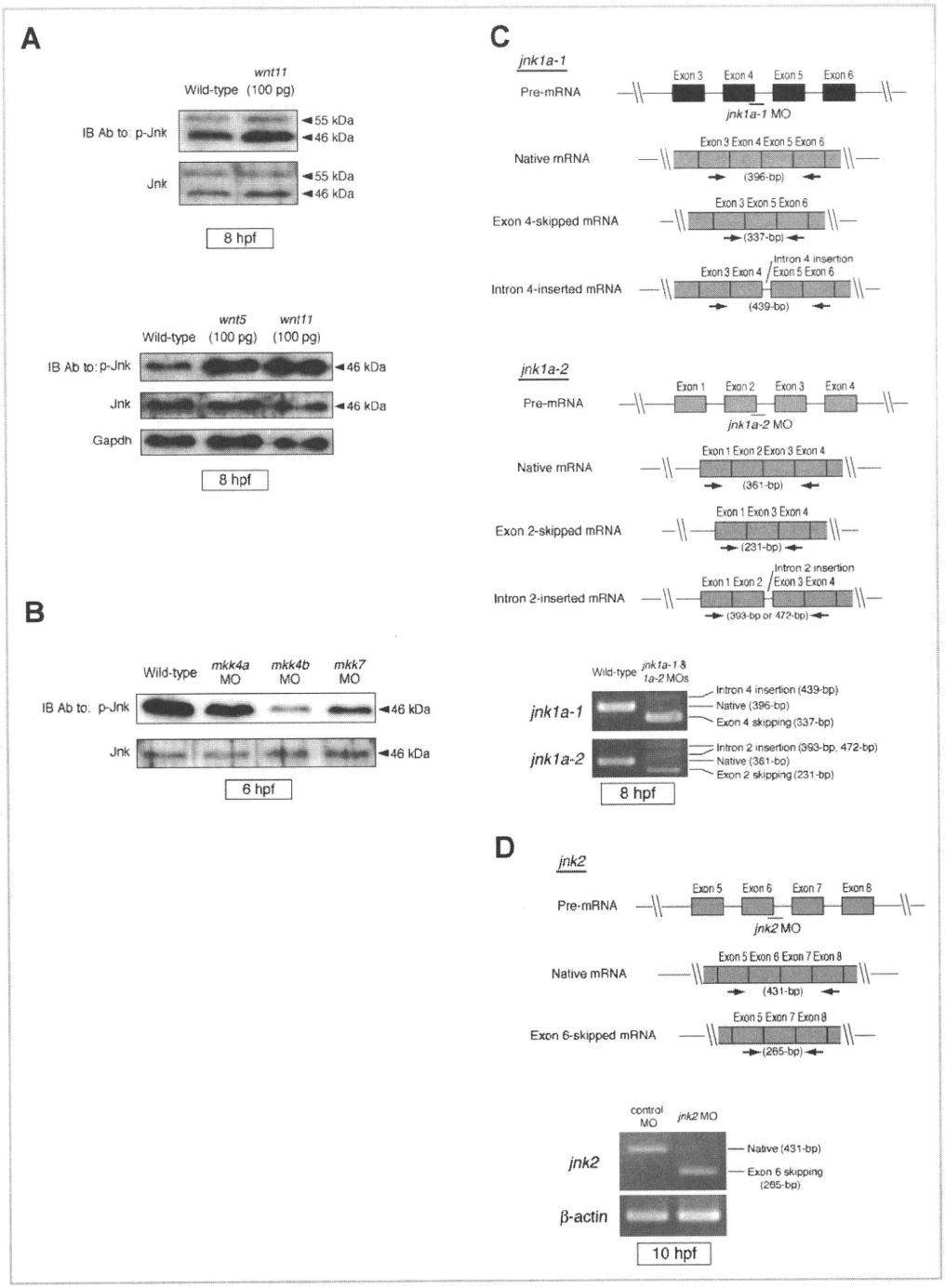

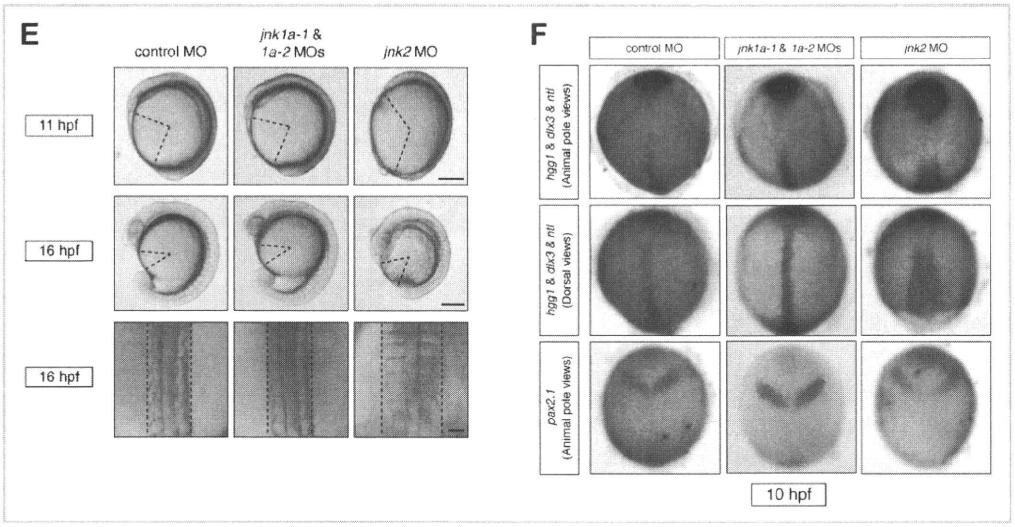

Fig. 3. Jnk2 is required for proper CE movements in zebrafish. A: Jnk is activated by *wnt11* or *wnt5* overexpression. Pooled extracts of 25 embryos overexpressing *wnt11* were analyzed by Western blotting (top). Levels of phospho-Jnk (p-Jnk) were increased compared to the control but total Jnk (55 and 46 kDa isoforms) was unchanged. Pooled extracts of 25 embryos overexpressing *wnt5* were analyzed by Western blotting (bottom). Gapdh, internal control. B: Markedly reduced Jnk phosphorylation in *mkk4b* morphants. Twenty-five embryos injected with 0.4 pmol of *mkk4a* MO, *mkk4b* MO, or *mkk7* MO were analyzed at the shield stage by Western blotting to detect Jnk and p-Jnk. C: Validation of *jnk1a* MOs. Schematic illustrations of the target sites of the *jnk1a-1* MO and *jnk1a-2* MO are shown in the top and center panels, respectively. Arrows represent the primer pairs used in the RT-PCR evaluation of MO efficacy. The bottom panel shows an RT-PCR analysis of the effects of these MOs on *jnk1a-1* and *jnk1a-2* expression. Total RNA was extracted at 8 hpf from untreated WT embryos, or WT embryos co-injected with *jnk1a-1* MO and *jnk1a-2* MO (0.8 pmol each). *Jnk1a-1* MO and *jnk1a-2* MO prevent correct splicing of *jnk1a-1* and *jnk1a-2* pre-mRNAs, respectively, resulting in a reading-frame shift and production of mutant proteins. D: Validation of *jnk2* MO. Top panel depicts the location of the target site of *jnk2* MO and the primer pairs used for RT-PCR. The bottom panel shows an RT-PCR analysis of the effect of *jnk2* MO. Total RNA was extracted from WT embryos injected with control MO (0.8 pmol) or *jnk2* MO (0.7 pmol). *Jnk2* MO induces defective splicing. E: Gross appearance of *jnk* morphants. Images of live embryos injected with control MO (0.8 pmol), *jnk1a-1* MO plus *jnk1a-2* MO (0.8 pmol each), or *jnk2* MO (0.7 pmol) were acquired at 11 and 16 hpf. These embryos are viewed laterally, with anterior to the top. *Jnk1* MOs cause no gross morphological defects, whereas *jnk2* morphants exhibit a shortening of body length. At 16 hpf, the notochord and somites are wider in the *jnk2* morphant than in the control (dorsal view). Scale bars = 200 μm (row 1); 200 μm (row 2); 50 μm (row 3). F: Impaired CE in *jnk2* morphants. *Jnk* morphants and controls were analyzed by whole-mount in situ hybridization for the expression of tissue-specific genes at the tailbud stage (10 hpf). *Jnk1a* morphants showed normal marker expression. In *jnk2* morphants, the position of the prechordal plate (*hgg1*) is more posterior and broader than in the control. Expression of *dlx3* (neuroectoderm) reveals a broader neural plate, and the notochord (*ntl*) is shorter and broader. The midbrain/hindbrain boundary (*pax2.1*) has expanded laterally.

of body length at 11, 16, and 24 hpf and exhibited broader notochords and somites at 16 hpf (Fig. 5A), reminiscent of the *mkk4b* morphant phenotype (Fig. 2B). With respect to marker expression patterns, the expression of the organizer marker *gsc* was not changed in *wnt11*-overexpressing embryos compared to control embryos injected with *egfp* mRNA (Fig. 5B, top). At the tailbud stage, *wnt11*-overexpressing embryos showed a more posteriorly positioned prechordal plate (*hgg1*), a wider neural plate (*dlx3*), a shorter and broader notochord (*ntl*), and a laterally expanded midbrain/hindbrain boundary (*pax2.1*) than did controls (Fig. 5B, bottom). These observations imply that the level of *wnt11* mRNA present critically influences CE.

MKK4B MORPHANTS SHOW INCREASED *WNT11* EXPRESSION IN THE ORGANIZER AND MARGIN REGIONS

We next used whole-mount in situ hybridization to localize the increased *wnt11* expression in Mkk4b-depleted embryos. During gastrulation in control MO-injected embryos, *wnt11* expression became prominent in the lateral and ventral germ ring (margin region) but was downregulated within the region of shield formation (i.e., the organizer) (Fig. 6A; 6 hpf). *Wnt11* expression near the margin persisted throughout gastrulation, although the staining intensity gradually decreased in the ventral region. *Wnt11* expression remained high in the dorsal region, which converges with the tailbud (Fig. 6A; 8 and 10 hpf). In contrast, during gastrulation in *mkk4b* morphants, *wnt11* expression was significantly increased in both the organizer and margin regions (Fig. 6A; 6 hpf). By late gastrulation, *wnt11* expression was strongly upregulated in all domains (Fig. 6A; 8 and 10 hpf). On the other hand, the expression pattern of *wnt5* in *mkk4b* morphants matched that of controls (Fig. 6B).

IMPAIRED MKK4B FUNCTION PROMOTES *WNT11* TRANSACTIVATION IN A NON-CELL-AUTONOMOUS MANNER

To determine whether *wnt11* was a direct transcriptional target of Mkk4b-Jnk signaling, we generated small clones of *mkk4b*-deficient zebrafish cells within whole embryos by co-injecting *mkk4b* MO together with *egfp* mRNA into one blastomere of a 32- or 64-cell embryo (Fig. 7A). We subsequently examined the location of the EGFP-labeled descendant cells at the shield stage (Fig. 7B, top row) and analyzed *wnt11* expression pattern by whole-mount in situ hybridization (Fig. 7B, bottom row). *Wnt11* expression was significantly elevated even in the embryonic region that did not overlap with the lineage label marking the progeny of *mkk4b* MO-

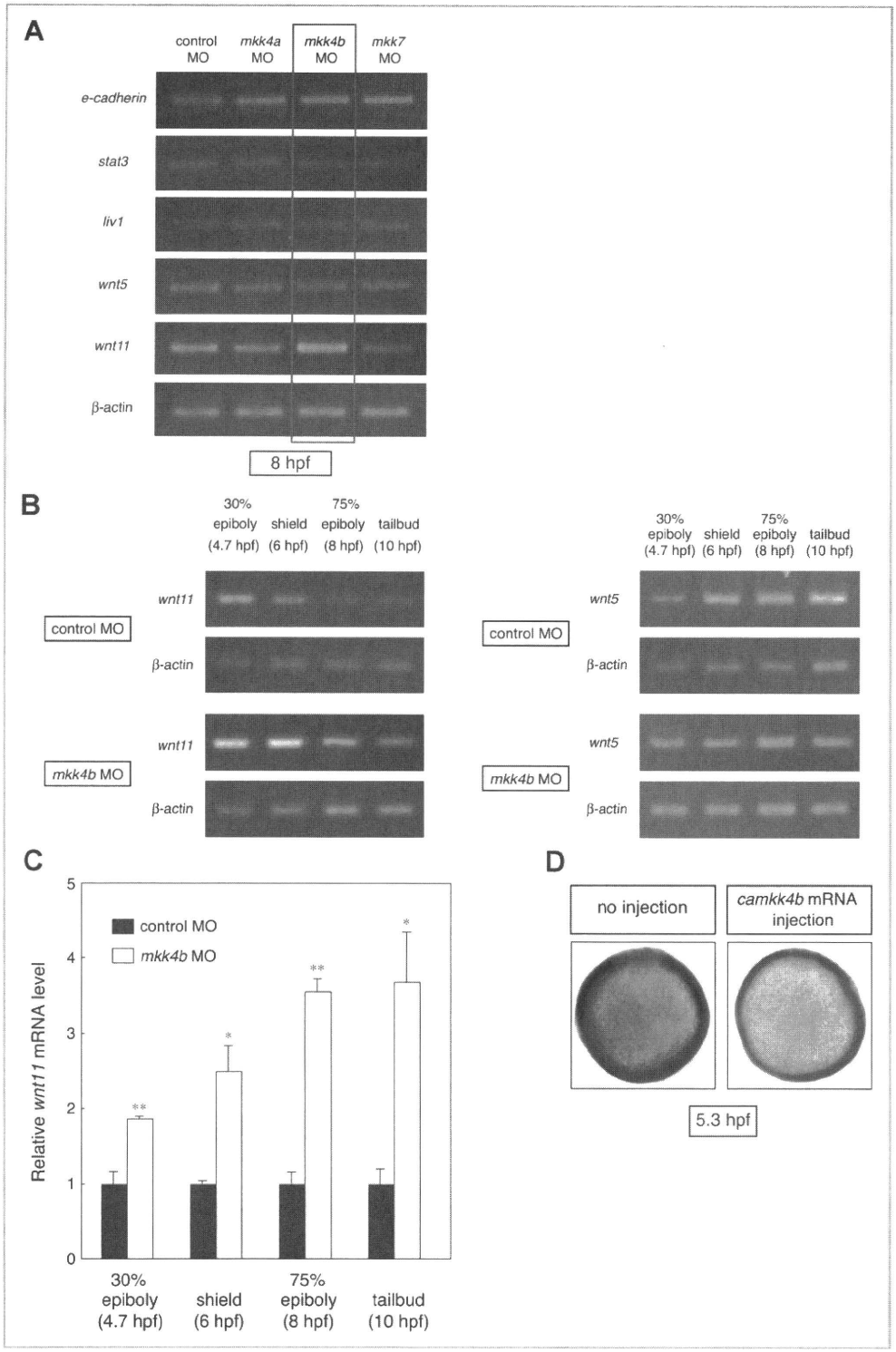

Fig. 4. Identification of *wnt11* as a downstream component of Mkk4b–Jnk signaling in the non-canonical Wnt pathway. A: Specific upregulation of *wnt11* in *mkk4b* morphants. Total RNA was isolated from control, *mkk4a*, *mkk4b*, and *mkk7* morphants at the 75% epiboly stage (8 hpf) and subjected to RT-PCR to detect expression of the indicated mRNAs. *β-Actin*, internal control. B: Upregulation of *wnt11* but not *wnt5* in *mkk4b* morphants throughout early embryogenesis. Total RNA was isolated from control and *mkk4b* morphants at the indicated stages and subjected to RT-PCR to detect expression of *wnt11* (left) and *wnt5* (right) mRNAs. C: Quantitative RT-PCR analysis of *wnt11* mRNA expression in *mkk4b* morphants. For all quantitative PCR experiments, *wnt11* cDNA amplification was standardized to the amplification of *β-actin* cDNA. *Wnt11* expression in *mkk4b* morphants was normalized to that in controls (assigned an arbitrary value of 1). Data shown are the mean ± SEM of three independent experiments ($^{*}P < 0.05$; $^{**}P < 0.01$ vs. control). D: Mkk4b–Jnk signaling represses *wnt11* expression. WT embryos were left untreated or injected with *camkk4b* mRNA (40 pg) and subjected to whole-mount in situ hybridization to detect *wnt11* at the 50% epiboly stage (5.3 hpf; animal pole views). Decreased *wnt11* expression was observed in *camkk4b*-overexpressing embryos (right) compared with uninjected embryos (left).

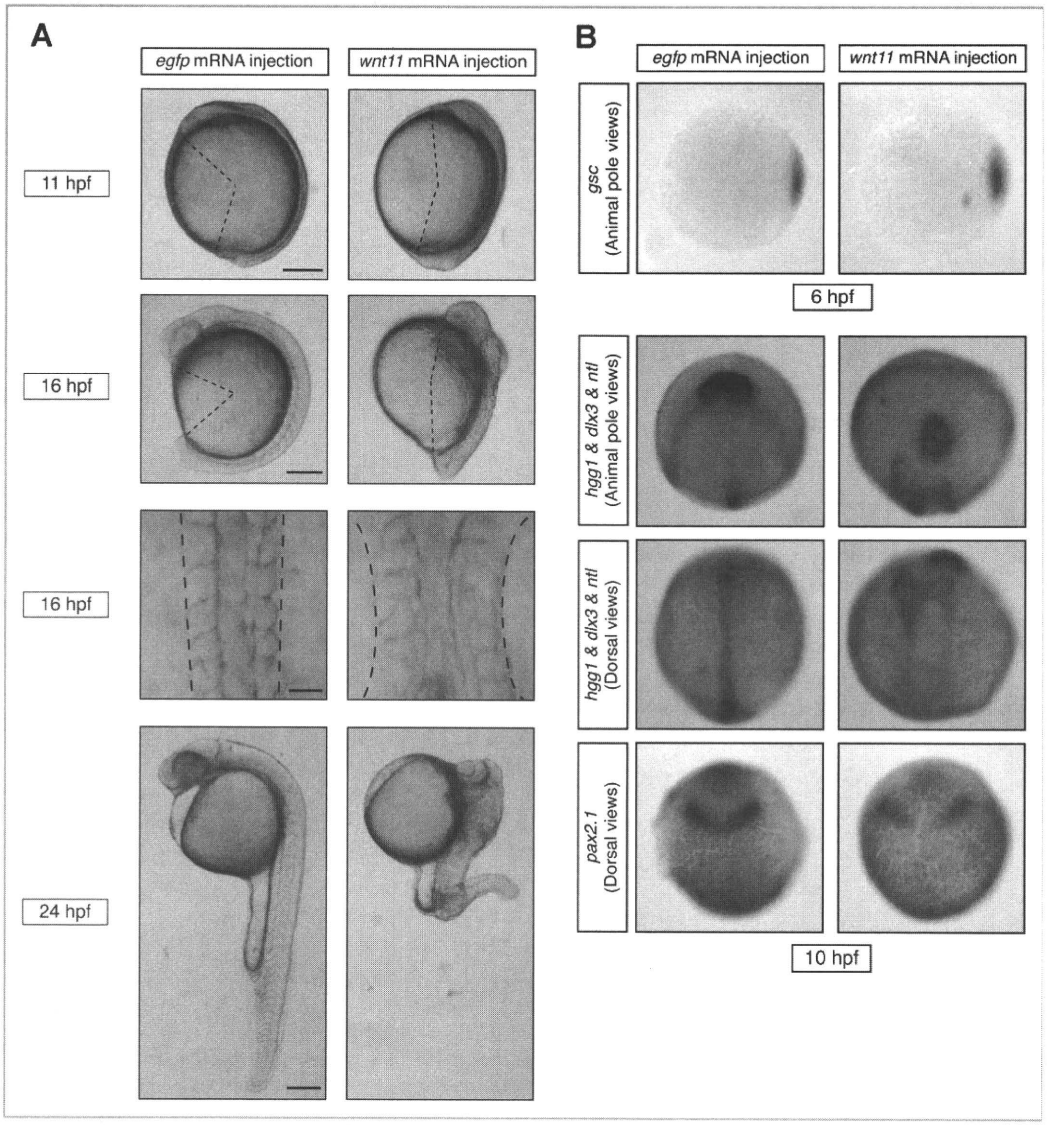

Fig. 5. Overexpression of *wnt11* induces CE abnormalities. A: Altered gross appearance. WT embryos were injected with either *egfp* mRNA (100 pg; control) or *wnt11* mRNA (75 pg), and the gross phenotype of the embryos was examined at 11, 16, and 24 hpf (rows 1, 2, and 4, respectively). These embryos are viewed laterally, with the anterior to the top. A shortening of body length can be seen as early as 11 hpf in the *wnt11*-overexpressing embryos. Row 3 shows that the notochord and somites are wider in the *wnt11*-overexpressing embryos than in the controls at 16 hpf (dorsal view). Scale bars = 200 μm (row 1); 200 μm (row 2); 50 μm (row 3); 200 μm (row 4). B: Impaired CE in *wnt11*-overexpressing embryos. WT embryos were injected with *egfp* or *wnt11* mRNA (100 pg), and analyzed by whole-mount in situ hybridization for the expression of tissue-specific genes at the shield stage (6 hpf) and the tailbud stage (10 hpf). The expression pattern of the organizer marker *gsc* is similar in the *wnt11*-overexpressing embryos and controls. However, the position of the prechordal plate (*hgg1*) is more posterior in *wnt11*-overexpressing embryos compared to the control. Expression of *dlx3* (neuroectoderm) reveals a broader neural plate, and the notochord (*ntl*) is shorter and broader. The midbrain/hindbrain boundary (*pax2.1*) has expanded laterally.

injected cells (Fig. 7B). Thus, activation of the Mkk4b–Jnk signaling pathway in zebrafish embryos represses *wnt11* expression in a non-cell-autonomous fashion.

Taken together, our findings suggest that the suppression of *wnt11* transcription by Jnk activation is important for the precise regulation of vertebrate CE, and establish a model in which non-canonical Wnt signaling leading to Jnk activation represses expression of the CE-triggering ligand Wnt11 (Fig. S7).

DISCUSSION

In this study, we examined the role of Jnk signaling during the early embryogenesis of zebrafish by carrying out MO-mediated knock-down of the orthologs of the *mkk4* and *mkk7* genes. We found that *mkk4a* MO-injected zebrafish embryos had no phenotype (Fig. S4B,C), whereas *mkk4b* MO-injected embryos exhibited axial tissues that were abnormally short and wide due to defective CE

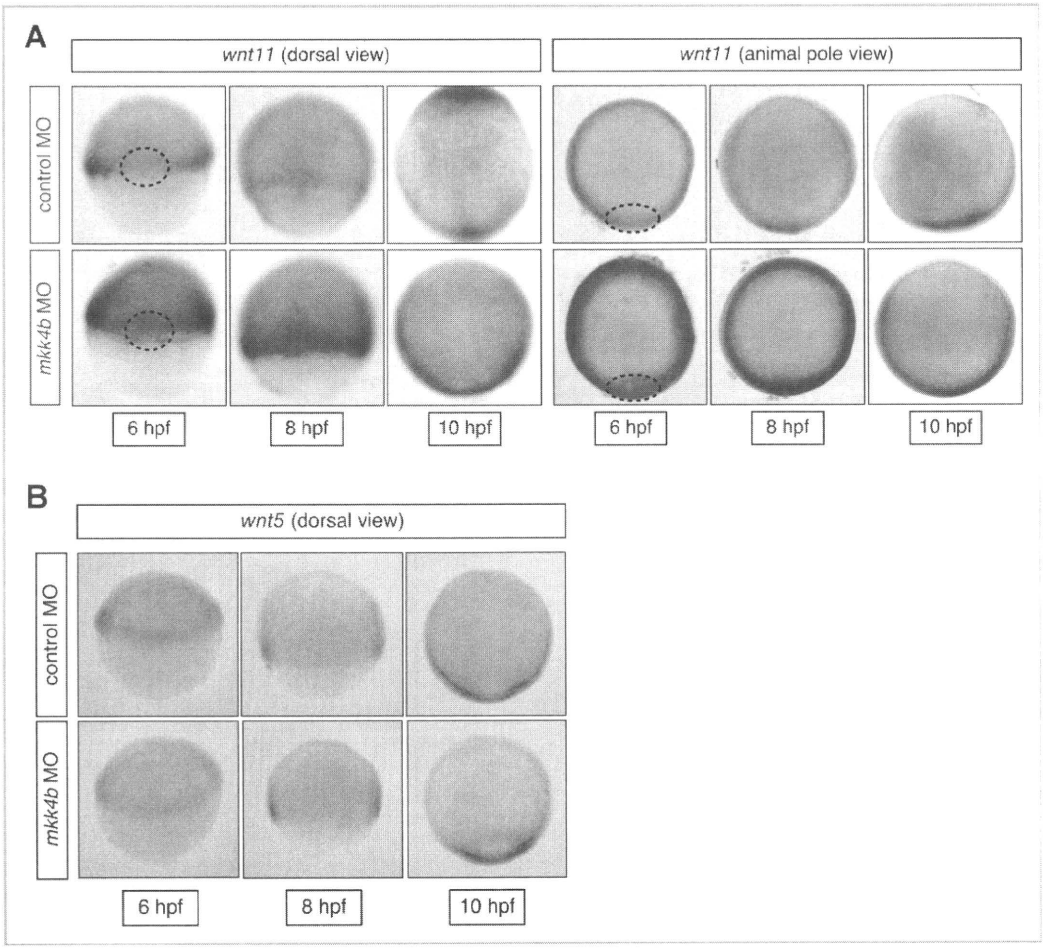

Fig. 6. Elevated expression of *wnt11* in the organizer and margin regions of Mkk4b-depleted embryos. A: Localization of increased *wnt11* expression in *mkk4b* morphants. Whole-mount in situ hybridization was used to monitor *wnt11* expression in developing control and *mkk4b* morphants from the shield stage (6 hpf) to tailbud stage (10 hpf). Two views are shown as indicated, with dashed lines outlining the boundaries of the organizer region. B: Localization of *wnt5* expression in *mkk4b* morphants. Whole-mount in situ hybridization was used to monitor *wnt5* expression in developing control and *mkk4b* morphants from the shield stage (6 hpf) to tailbud stage (10 hpf). *Wnt5* showed the same expression pattern in control and *mkk4b* morphants.

(Fig. 2B–E). These observations suggest that Mkk4b is functionally redundant with Mkk4a and can compensate for its loss during gastrulation, but that Mkk4a cannot compensate for a lack of Mkk4b. *Mkk7* morphants had no phenotype during gastrulation but showed abnormal somite morphologies during segmentation (Fig. 2H–J). Mkk7 is thus critical for a slightly later stage of development.

Recently, Rui et al. [2007] demonstrated that zebrafish *mkk4a-s* plays an important role in dorsoventral patterning in zebrafish blastulas. These authors reported that *mkk4a-s* knockdown with a translation-blocking MO prior to gastrulation reduced the expression of dorsal markers but expanded the expression of ventral markers. In our study, we performed *mkk4a-l* knockdown with translation-blocking MO but could not detect any alteration to the expression of the dorsal marker *gsc* (Fig. S8). This discrepancy implies that there is functional diversity between the two splicing isoforms of *mkk4a*. The results of our study, together with those of Rui et al., reinforce the idea that Jnk signaling plays multiple roles in major developmental processes, including the specification of the dorsoventral axis, cell movements required during gastrulation, and somite morphogenesis.

Our previous studies of disruption of the *mkk4* and *mkk7* genes in murine ES cells revealed that Mkk4 and Mkk7 preferentially phosphorylate the Tyr and Thr residues, respectively, within the Thr-Pro-Tyr motif of Jnk [Kishimoto et al., 2003]. In this study, we expressed zebrafish Mkk4 and Mkk7 in mouse ES cells and obtained results indicating that these Mapks also differ in their biochemical properties (Fig. 1C). These data strongly suggest that the use of Jnk activation as a molecular switch has been evolutionarily conserved from teleosts to mammals. In zebrafish, loss of Mkk4b leads to severe defects in CE movements during gastrulation, whereas our *mkk7* morphants had no phenotype during gastrulation (Fig. 2D,I). These observations indicate that *mkk4* has a more prominent role than *mkk7* in early embryogenesis. Consistent with this hypothesis, $mkk4^{-/-}$ mouse embryos die earlier than $mkk7^{-/-}$ embryos [Nishina et al., 1999; Wada et al., 2004]. This conserved functional

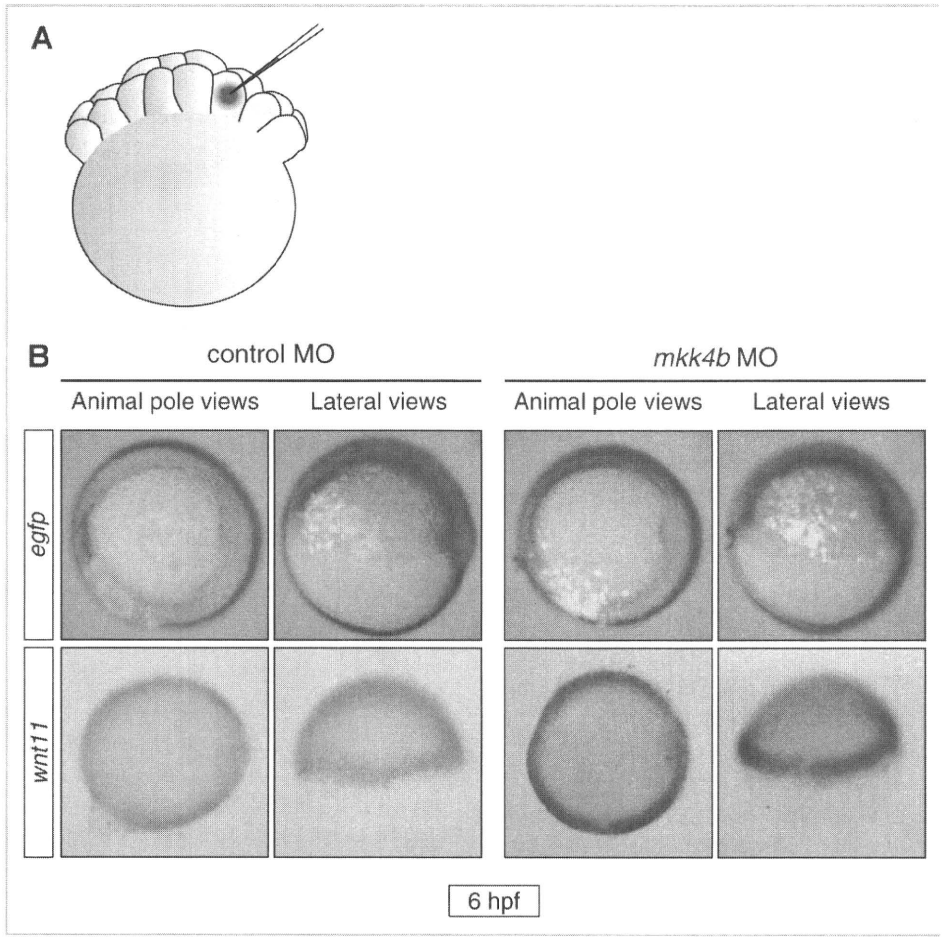

Fig. 7. Abrogation of Mkk4b function induces elevated expression of *wnt11* in a non-cell-autonomous manner. A: Schematic representation of MO microinjection into one cell of a 32- or 64-cell zebrafish embryo. B: Control MO (0.4 pmol) or *mkk4b* MO (0.4 pmol) was injected into one cell of a 32- or 64-cell embryo to generate randomly distributed *mkk4b*-knockdown cell clones. *Egfp* mRNA was co-injected as a cell lineage tracer. Top, EGFP-labeled cells were observed at the shield stage by fluorescence microscopy using a halogen lamp and blue light. Bottom, *wnt11* expression was monitored in developing control and *mkk4b* morphants at the shield stage by whole-mount in situ hybridization. Two views are shown, with dorsal to the right.

diversity of Mapks may be related to the need to activate Jnk at different times and locations during early development. Indeed, we found that Mkk4b depletion reduced Jnk phosphorylation more dramatically than did Mkk7 depletion, at least at the shield stage (Fig. 3B). Alternatively, the functional properties of Mkk4b–Jnk and Mkk7–Jnk signaling modules may be governed in part by scaffold proteins such as the Jnk-interacting proteins (JIPs) that confer specificity to kinase actions [Whitmarsh, 2006].

$Jnk1^{-/-}jnk2^{-/-}$ mice die at about E11 with defective neural tube morphogenesis [Kuan et al., 1999]. Based on our results in zebrafish, we speculate that the failure to close the neural tube in $jnk1^{-/-}jnk2^{-/-}$ mice may be due to defective CE in the neural plate. In support of this idea, disruption of non-canonical Wnt pathway genes (such as *dishevelled*) in *Xenopus* inhibits CE in the neural plate and results in abnormal, widely spaced neural folds that do not close [Copp et al., 2003]. Invertebrate development may also rely on Jnk-mediated events that share molecular similarities with vertebrate CE. In *Drosophila*, dJnk (Basket) is activated by dJnkk (Hemipterous), a homolog of vertebrate Mkk7 [Glise et al., 1995; Riesgo-Escovar et al., 1996; Sluss et al., 1996]. *Basket* and *hemipterous* are important for morphogenesis, and loss of function of either gene inhibits dorsal closure [Glise et al., 1995; Riesgo-Escovar et al., 1996; Sluss et al., 1996]. These findings emphasize the notion that Jnk activation is utilized in parallel morphogenetic events among widely divergent species.

Signals initiated by non-canonical Wnt ligands such as Wnt11 and Wnt5 are important for: vertebrate morphogenetic processes that require directed cell movements; cell-cell adhesion; and the establishment of cell polarity. Zebrafish with mutations in *wnt5* (*ppt*) or *wnt11* (*slb*) exhibit defects that reduce CE without affecting cell fate [Heisenberg et al., 2000; Kilian et al., 2003]. The *slb* mutant shows more anterior CE defects, including a shortened and broadened body axis at the end of gastrulation and a slight fusion of the eyes (cyclopia) at later developmental stages. In contrast, the Wnt5 protein functions in posterior regions. The *ppt* mutant exhibits a shortened body axis and compressed tail, whereas the position of the eyes is only mildly affected. These observations indicate that Wnt11 and Wnt5 possess distinct and non-redundant functions in regulating zebrafish gastrulation, which may be accounted for by differences in spatiotemporal expression. Although both *wnt5* and

wnt11 are expressed in the germ ring at the shield stage, *wnt11* is specifically expressed in anterior tissues at the end of gastrulation, whereas *wnt5* is specifically expressed in posterior mesendodermal tissues (Fig. 6) [Heisenberg et al., 2000; Kilian et al., 2003]. Our study demonstrates that Mkk4b–Jnk signaling precisely regulates *wnt11* transcription. This Mkk4b–Jnk-mediated control may contribute to the mechanisms segregating *wnt11* and *wnt5* expression domains during late gastrulation.

In *Drosophila*, a role for Dpp in dorsal closure during early morphogenesis has been clearly established [Hou et al., 1997; Riesgo-Escovar and Hafen, 1997]. During dorsal closure, Jnk activates the expression of *dpp* in leading-edge epithelial cells, and Dpp subsequently acts as a secreted signal that controls the elongation of lateral epidermis in a paracrine fashion [Reed et al., 2001]. Our analyses demonstrate that Mkk4b–Jnk signaling regulates *wnt11* expression during zebrafish gastrulation in a non-cell-autonomous manner (Fig. 7). Our results raise the possibility that, like *Drosophila* dorsal closure, normal vertebrate CE movements depend on Jnk signaling that regulates the expression of a secreted signaling molecule capable of promoting concerted movements of neighboring cells (Fig. S7).

Our proposed model of CE movement regulation by *wnt11* expression can be summarized as follows: In normal zebrafish embryos, activated Mkk4b transmits a signal leading to Jnk activation. This activated Jnk may induce secreted factor X, which exerts moderate suppression of *wnt11* transcription in neighboring organizer and margin cells, and results in proper co-ordination of CE. In *mkk4b* morphants, however, JNK activation is blocked such that the expression of factor X is downregulated. As a result, *wnt11* is expressed at an abnormally high level that may impair CE (Fig. 7). We undertook preliminary studies to examine whether the *mkk4b* morphant phenotype could be suppressed by a low dose of *wnt11* MO, but found that rescue did not occur (data not shown). This inability to rescue the CE defect may be due to a failure to strictly control the expression pattern and amount of *wnt11* expression, since Wnt11 levels and localization must be tightly regulated for normal embryonic development [Heisenberg et al., 2000].

A previous study demonstrated that Bmp activity regulates CE movements during zebrafish gastrulation [Myers et al., 2002]. This report prompted us to investigate whether zebrafish Bmp2 and Bmp4 (homologs of *Drosophila* Dpp) function downstream of the Mkk4b–Jnk signaling cascade. However, expression levels of *bmp2* and *bmp4* were not downregulated in Mkk4b-depleted embryos (data not shown). Future identification of secreted factor(s) responsible for the transmission of Jnk signals to neighboring cells may provide insight into the complex mechanisms controlling vertebrate CE.

Our proposed model postulates that *wnt11* expression is under precise spatiotemporal control during zebrafish development. Previous studies have shown that Wnt11 expression in zebrafish starts in the dorsal part of the blastoderm margin at the oblong stage, and that the entire margin becomes $Wnt11^{+}$ by the late blastula stage [Makita et al., 1998]. Our present work shows that, at the onset of gastrulation, *wnt11* is highly expressed around the circumference of the germ ring, with slightly reduced expression in the region of the organizer (Fig. 6A). It has been established that *wnt11* is expressed predominantly in epiblast cells of the germ ring (ectodermal germ layer), whereas ingressing hypoblast cells (mesendodermal germ layer) show no detectable *wnt11* expression [Makita et al., 1998; Ulrich et al., 2003]. This profile of early *wnt11* expression in zebrafish is virtually identical to that seen in *Xenopus* [Ku and Melton, 1993]. Taken together, these results suggest an evolutionary conservation of *wnt11* function during gastrulation, and a prominent role for the control of *wnt11* expression by Jnk signaling.

ACKNOWLEDGMENTS

We thank numerous members of the Nishina and Katada Laboratories for their helpful discussions and critical comments on the manuscript. This work was partly supported by a Grant-in-Aid for Scientific Research on a Priority Area from the Ministry of Education, Culture, Sports, Science and Technology of Japan. This work was also supported by grants from the Japan Society for the Promotion of Science, the Ministry of Education, Culture, Sports, Science and Technology of Japan, and the Ministry of Health, Labor and Welfare of Japan.

REFERENCES

Asaoka Y, Mano H, Kojima D, Fukada Y. 2002. Pineal expression-promoting element (PIPE), a cis-acting element, directs pineal-specific gene expression in zebrafish. Proc Natl Acad Sci USA 99:15456–15461.

Chang L, Karin M. 2001. Mammalian MAP kinase signalling cascades. Nature 410:37–40.

Copp AJ, Greene ND, Murdoch JN. 2003. Dishevelled: Linking convergent extension with neural tube closure. Trends Neurosci 26:453–455.

Davis RJ. 2000. Signal transduction by the JNK group of MAP kinases. Cell 103:239–252.

Derijard B, Hibi M, Wu IH, Barrett T, Su B, Deng T, Karin M, Davis RJ. 1994. JNK1: A protein kinase stimulated by UV light and Ha-Ras that binds and phosphorylates the c-Jun activation domain. Cell 76:1025–1037.

Fleming Y, Armstrong CG, Morrice N, Paterson A, Goedert M, Cohen P. 2000. Synergistic activation of stress-activated protein kinase 1/c-Jun N-terminal kinase (SAPK1/JNK) isoforms by mitogen-activated protein kinase kinase 4 (MKK4) and MKK7. Biochem J 352(Pt 1): 145–154.

Ganiatsas S, Kwee L, Fujiwara Y, Perkins A, Ikeda T, Labow MA, Zon LI. 1998. SEK1 deficiency reveals mitogen-activated protein kinase cascade cross-regulation and leads to abnormal hepatogenesis. Proc Natl Acad Sci USA 95:6881–6886.

Glise B, Bourbon H, Noselli S. 1995. Hemipterous encodes a novel *Drosophila* MAP kinase kinase, required for epithelial cell sheet movement. Cell 83:451–461.

Habas R, Kato Y, He X. 2001. Wnt/Frizzled activation of Rho regulates vertebrate gastrulation and requires a novel Formin homology protein Daam1. Cell 107:843–854.

Habas R, Dawid IB, He X. 2003. Coactivation of Rac and Rho by Wnt/Frizzled signaling is required for vertebrate gastrulation. Genes Dev 17:295–309.

Heisenberg CP, Tada M, Rauch GJ, Saude L, Concha ML, Geisler R, Stemple DL, Smith JC, Wilson SW. 2000. Silberblick/Wnt11 mediates convergent extension movements during zebrafish gastrulation. Nature 405:76–81.

Hou XS, Goldstein ES, Perrimon N. 1997. *Drosophila* Jun relays the Jun amino-terminal kinase signal transduction pathway to the Decapentaplegic signal transduction pathway in regulating epithelial cell sheet movement. Genes Dev 11:1728–1737.

Kallunki T, Su B, Tsigelny I, Sluss HK, Derijard B, Moore G, Davis R, Karin M. 1994. JNK2 contains a specificity-determining region responsible for efficient c-Jun binding and phosphorylation. Genes Dev 8:2996–3007.

Keller R. 2002. Shaping the vertebrate body plan by polarized embryonic cell movements. Science 298:1950–1954.

Kilian B, Mansukoski H, Barbosa FC, Ulrich F, Tada M, Heisenberg CP. 2003. The role of Ppt/Wnt5 in regulating cell shape and movement during zebrafish gastrulation. Mech Dev 120:467–476.

Kim GH, Han JK. 2005. JNK and ROKalpha function in the noncanonical Wnt/RhoA signaling pathway to regulate Xenopus convergent extension movements. Dev Dyn 232:958–968.

Kimmel CB, Ballard WW, Kimmel SR, Ullmann B, Schilling TF. 1995. Stages of embryonic development of the zebrafish. Dev Dyn 203:253–310.

Kishimoto H, Nakagawa K, Watanabe T, Kitagawa D, Momose H, Seo J, Nishitai G, Shimizu N, Ohata S, Tanemura S, Asaka S, Goto T, Fukushi H, Yoshida H, Suzuki A, Sasaki T, Wada T, Penninger JM, Nishina H, Katada T. 2003. Different properties of SEK1 and MKK7 in dual phosphorylation of stress-induced activated protein kinase SAPK/JNK in embryonic stem cells. J Biol Chem 278:16595–16601.

Ku M, Melton DA. 1993. Xwnt-11: A maternally expressed Xenopus wnt gene. Development 119:1161–1173.

Kuan CY, Yang DD, Samanta Roy DR, Davis RJ, Rakic P, Flavell RA. 1999. The Jnk1 and Jnk2 protein kinases are required for regional specific apoptosis during early brain development. Neuron 22:667–676.

Lawler S, Fleming Y, Goedert M, Cohen P. 1998. Synergistic activation of SAPK1/JNK1 by two MAP kinase kinases in vitro. Curr Biol 8:1387–1390.

Link V, Shevchenko A, Heisenberg CP. 2006. Proteomics of early zebrafish embryos. BMC Dev Biol 6:1.

Makita R, Mizuno T, Koshida S, Kuroiwa A, Takeda H. 1998. Zebrafish wnt11: Pattern and regulation of the expression by the yolk cell and No tail activity. Mech Dev 71:165–176.

Mohit AA, Martin JH, Miller CA. 1995. p493F12 kinase: A novel MAP kinase expressed in a subset of neurons in the human nervous system. Neuron 14:67–78.

Myers DC, Sepich DS, Solnica-Krezel L. 2002. Bmp activity gradient regulates convergent extension during zebrafish gastrulation. Dev Biol 243:81–98.

Nishina H, Fischer KD, Radvanyi L, Shahinian A, Hakem R, Rubie EA, Bernstein A, Mak TW, Woodgett JR, Penninger JM. 1997. Stress-signalling kinase Sek1 protects thymocytes from apoptosis mediated by CD95 and CD3. Nature 385:350–353.

Nishina H, Vaz C, Billia P, Nghiem M, Sasaki T, De la Pompa JL, Furlonger K, Paige C, Hui C, Fischer KD, Kishimoto H, Iwatsubo T, Katada T, Woodgett JR, Penninger JM. 1999. Defective liver formation and liver cell apoptosis in mice lacking the stress signaling kinase SEK1/MKK4. Development 126:505–516.

Nishitai G, Shimizu N, Negishi T, Kishimoto H, Nakagawa K, Kitagawa D, Watanabe T, Momose H, Ohata S, Tanemura S, Asaka S, Kubota J, Saito R, Yoshida H, Mak TW, Wada T, Penninger JM, Azuma N, Nishina H, Katada T. 2004. Stress induces mitochondria-mediated apoptosis independent of SAPK/JNK activation in embryonic stem cells. J Biol Chem 279:1621–1626.

Okuda Y, Yoda H, Uchikawa M, Furutani-Seiki M, Takeda H, Kondoh H, Kamachi Y. 2006. Comparative genomic and expression analysis of group B1 sox genes in zebrafish indicates their diversification during vertebrate evolution. Dev Dyn 235:811–825.

Reed BH, Wilk R, Lipshitz HD. 2001. Downregulation of Jun kinase signaling in the amnioserosa is essential for dorsal closure of the *Drosophila* embryo. Curr Biol 11:1098–1108.

Riesgo-Escovar JR, Hafen E. 1997. *Drosophila* Jun kinase regulates expression of decapentaplegic via the ETS-domain protein Aop and the AP-1 transcription factor DJun during dorsal closure. Genes Dev 11:1717–1727.

Riesgo-Escovar JR, Jenni M, Fritz A, Hafen E. 1996. The *Drosophila* Jun-N-terminal kinase is required for cell morphogenesis but not for DJun-dependent cell fate specification in the eye. Genes Dev 10:2759–2768.

Rui Y, Xu Z, Xiong B, Cao Y, Lin S, Zhang M, Chan SC, Luo W, Han Y, Lu Z, Ye Z, Zhou HM, Han J, Meng A, Lin SC. 2007. A beta-catenin-independent dorsalization pathway activated by Axin/JNK signaling and antagonized by aida. Dev Cell 13:268–282.

Seifert JR, Mlodzik M. 2007. Frizzled/PCP signalling: A conserved mechanism regulating cell polarity and directed motility. Nat Rev Genet 8:126–138.

Shinya M, Eschbach C, Clark M, Lehrach H, Furutani-Seiki M. 2000. Zebrafish Dkk1, induced by the pre-MBT Wnt signaling, is secreted from the prechordal plate and patterns the anterior neural plate. Mech Dev 98:3–17.

Sluss HK, Han Z, Barrett T, Goberdhan DC, Wilson C, Davis RJ, Ip YT. 1996. A JNK signal transduction pathway that mediates morphogenesis and an immune response in *Drosophila*. Genes Dev 10:2745–2758.

Solnica-Krezel L. 2005. Conserved patterns of cell movements during vertebrate gastrulation. Curr Biol 15:R213–R228.

Tada M, Concha ML, Heisenberg CP. 2002. Non-canonical Wnt signalling and regulation of gastrulation movements. Semin Cell Dev Biol 13:251–260.

Thisse C, Thisse B, Schilling TF, Postlethwait JH. 1993. Structure of the zebrafish snail1 gene and its expression in wild-type, spadetail and no tail mutant embryos. Development 119:1203–1215.

Tournier C, Dong C, Turner TK, Jones SN, Flavell RA, Davis RJ. 2001. MKK7 is an essential component of the JNK signal transduction pathway activated by proinflammatory cytokines. Genes Dev 15:1419–1426.

Ulrich F, Concha ML, Heid PJ, Voss E, Witzel S, Roehl H, Tada M, Wilson SW, Adams RJ, Soll DR, Heisenberg CP. 2003. Slb/Wnt11 controls hypoblast cell migration and morphogenesis at the onset of zebrafish gastrulation. Development 130:5375–5384.

Ura S, Nishina H, Gotoh Y, Katada T. 2007. Activation of the c-Jun N-terminal kinase pathway by MST1 is essential and sufficient for the induction of chromatin condensation during apoptosis. Mol Cell Biol 27:5514–5522.

Wada T, Joza N, Cheng HY, Sasaki T, Kozieradzki I, Bachmaier K, Katada T, Schreiber M, Wagner EF, Nishina H, Penninger JM. 2004. MKK7 couples stress signalling to G2/M cell-cycle progression and cellular senescence. Nat Cell Biol 6:215–226.

Watanabe T, Nakagawa K, Ohata S, Kitagawa D, Nishitai G, Seo J, Tanemura S, Shimizu N, Kishimoto H, Wada T, Aoki J, Arai H, Iwatsubo T, Mochita M, Satake M, Ito Y, Matsuyama T, Mak TW, Penninger JM, Nishina H, Katada T. 2002. SEK1/MKK4-mediated SAPK/JNK signaling participates in embryonic hepatoblast proliferation via a pathway different from NF-kappaB-induced anti-apoptosis. Dev Biol 250:332–347.

Westerfield M. 1994. The Zebrafish Book: A Guide for the Laboratory Use of Zebrafish (*Branchydanio rerio*), Institute of Neuroscience. Eugene, OR: University of Oregon.

Whitmarsh AJ. 2006. The JIP family of MAPK scaffold proteins. Biochem Soc Trans 34:828–832.

Whitmarsh AJ, Cavanagh J, Tournier C, Yasuda J, Davis RJ. 1998. A mammalian scaffold complex that selectively mediates MAP kinase activation. Science 281:1671–1674.

Yamanaka H, Moriguchi T, Masuyama N, Kusakabe M, Hanafusa H, Takada R, Takada S, Nishida E. 2002. JNK functions in the non-canonical Wnt pathway to regulate convergent extension movements in vertebrates. EMBO Rep 3:69–75.

Yamashita S, Miyagi C, Fukada T, Kagara N, Che YS, Hirano T. 2004. Zinc transporter LIVI controls epithelial-mesenchymal transition in zebrafish gastrula organizer. Nature 429:298–302.

Yang D, Tournier C, Wysk M, Lu HT, Xu J, Davis RJ, Flavell RA. 1997. Targeted disruption of the MKK4 gene causes embryonic death, inhibition of c-Jun NH2-terminal kinase activation, and defects in AP-1 transcriptional activity. Proc Natl Acad Sci USA 94:3004–3009.

Filamin associates with stress signalling kinases MKK7 and MKK4 and regulates JNK activation

Kentaro NAKAGAWA*†‡[1], Misato SUGAHARA‡[1], Tokiwa YAMASAKI*‡[1], Hiroaki KAJIHO‡, Shinya TAKAHASHI*‡, Jun HIRAYAMA§, Yasuhiro MINAMI||, Yasutaka OHTA¶, Toshio WATANABE**, Yutaka HATA†, Toshiaki KATADA‡ and Hiroshi NISHINA*[2]

*Department of Developmental and Regenerative Biology, Medical Research Institute, Tokyo Medical and Dental University, 1-5-45 Yushima, Bunkyo-ku, Tokyo 113-8510, Japan, †Department of Medical Biochemistry, Graduate School of Medicine, Tokyo Medical and Dental University, 1-5-45 Yushima, Bunkyo-ku, Tokyo 113-8519, Japan, ‡Department of Physiological Chemistry, Graduate School of Pharmaceutical Sciences, University of Tokyo, 7-3-1 Hongo, Bunkyo-ku, Tokyo 113-0033, Japan, §Medical Top Track Program, Medical Research Institute, Tokyo Medical and Dental University, 1-5-45 Yushima, Bunkyo-ku, Tokyo 113-8510, Japan, ||Department of Physiology and Cell Biology, Graduate School of Medicine, Kobe University, 7-5-1, Kusunoki-cho, Chuo-ku, Kobe 650-0017, Japan, ¶Department of Medicine, Brigham and Women's Hospital, Harvard Medical School, Boston, Massachusetts 02115-2248, U.S.A., and **Department of Biological Sciences, Graduate School of Humanities and Sciences, Nara Women's University, Nara 630-8506, Japan

SAPK/JNK (stress-activated protein kinase/c-Jun N-terminal kinase) belongs to the MAPK (mitogen-activated protein kinase) family and is important in many biological contexts. JNK activation is regulated by phosphorylation of specific tyrosine and threonine residues sequentially catalysed by MKK4 and MKK7, which are both dual-specificity MAPKKs (MAPK kinases). Previously, we reported that tyrosine-phosphorylation of JNK by MKK4 precedes threonine-phosphorylation by MKK7, and that both are required for synergistic JNK activation. In the present study, we identify the actin-binding protein-280 (Filamin A) as a presumed 'binder' protein that can bind to MKK7, as well as to MKK4, connecting them in close proximity. We show that Filamin family members A, B and C interact with MKK4 and MKK7, but not with JNK. Filamin A binds to an N-terminal region (residues 31–60) present in the MKK7γ and MKK7β splice isoforms, but cannot bind to MKK7α which lacks these amino acids. This same N-terminal region is crucial for the intracellular co-localization of MKK7γ with actin stress fibres and Filamin A. Experiments using Filamin-A-deletion mutants revealed that the MKK7-binding region of Filamin A differs from its MKK4-binding region, and that MKK7γ (but not MKK7α) can form a complex with Filamin A and MKK4. Finally, we used Filamin-A-deficient cells to show that Filamin A enhances MKK7 activation and is important for synergistic stress-induced JNK activation *in vivo*. Thus Filamin A is a novel member of the group of scaffold proteins whose function is to link two MAPKKs together and promote JNK activation.

Key words: Filamin, c-Jun N-terminal kinase (JNK), mitogen-activated protein kinase kinase 4 (MKK4), mitogen-activated protein kinase kinase 7 (MKK7), stress-activated protein kinase (SAPK), stress-activated protein kinase/extracellular-signal-regulated kinase kinase 1 (SEK1).

INTRODUCTION

JNK (c-Jun N-terminal kinase) is a member of the family of MAPKs (mitogen-activated protein kinases), which are ubiquitously expressed and evolutionarily conserved. JNK is activated not only by many types of external stress, including changes in osmolarity, heat shock and UV-irradiation, but also by LPA (lysophosphatidic acid) and inflammatory cytokines. Activated JNK phosphorylates the transcription factors c-Jun, Jun D and ATF-2 (activating transcription factor 2) to regulate gene expression governing stress responses. JNK signalling is also involved in the normal physiological processes of cell proliferation, apoptosis, differentiation and cell migration [1,2].

Activation of JNK requires the phosphorylation of the tyrosine and threonine residues located in a threonine-proline-tyrosine motif in the activation loop between regions VII and VIII of the kinase domain. This phosphorylation is catalysed by two dual-specificity kinases, MKK4 (SEK1) and MKK7. MKK4 and MKK7 are MAPKKs (MAPK kinases) that are activated by various MAPKKKs (MAPKK kinases), including MLKs (mixed lineage protein kinases), MEKK1 {MEK [MAPK/ERK (extracellular-signal-regulated kinase) kinase] kinase}, TAK1 [TGF (transforming growth factor)-β-activated kinase 1] and ASK1 (apoptosis signal-regulating kinase) [1,2]. In-depth studies of JNK activation have shown that MKK4 preferentially phosphorylates the tyrosine residue of the threonine-proline-tyrosine motif, whereas MKK7 preferentially phosphorylates the threonine residue. Phosphorylation of both residues *in vitro* results in synergistic activation of JNK [3–5]. We obtained strong *in vivo* support for this latter activation mechanism from our studies of murine ES (embryonic stem) cells bearing disruptions of the *mkk4* and/or *mkk7* genes [6–8]. No JNK activation was observed in *mkk4*$^{-/-}$*mkk7*$^{-/-}$ ES cells [9]. In *mkk7*$^{-/-}$ ES cells, a severe impairment of JNK activation was observed that was accompanied by loss of phosphorylation of the threonine residue of JNK; however, there was no significant reduction in the phosphorylation of the tyrosine residue of JNK. In *mkk4*$^{-/-}$ ES cells, reductions in the phosphorylation of both the tyrosine and threonine residues of JNK were noted. These results indicated

Abbreviations used: Ab, antibody; CT, C-terminus; ES, embryonic stem; GFP, green fluorescent protein; GST, glutathione transferase; HA, haemagglutinin; HEK, human embryonic kidney; JNK, c-Jun N-terminal kinase; JIP, JNK-interacting protein; JLP, JNK-associated leucine-zipper protein; mAb, monoclonal antibody; MAPK, mitogen-activated protein kinase; MAPKK (MKK), MAPK kinase; MAPKKK, MAPKK kinase; MEKK1, MEK [MAPK/ERK (extracellular-signal-regulated kinase) kinase] kinase; MLK, mixed lineage protein kinase; SAPK, stress-activated protein kinase; JSAP1, JNK/SAPK-associated protein 1; TNF, tumour necrosis factor; TRAF2, TNF-receptor-associated factor.

[1] These authors contributed equally to the present study.

[2] To whom correspondence should be addressed (email nishina.dbio@mri.tmd.ac.jp).

that tyrosine phosphorylation by MKK4, followed by threonine phosphorylation by MKK7, leads to synergistic JNK activation in stress-stimulated ES cells. However, the molecular mechanism underlying the sequential phosphorylation of JNK by MKK4 and MKK7 remains to be elucidated.

Recent studies have shown that scaffold proteins mediate the structural and functional organization of a three-tier MAPK activation module which involves a MAPKKK, a MAPKK and a MAPK [10]. These MAPK-specific scaffold proteins link these kinases into a multienzyme complex and provide an insulated physical conduit through which signals from a MAPK can be transmitted to the appropriate spatiotemporal cellular loci. The scaffold proteins then modulate the signalling strength of their cognate MAPK module by regulating the amplitude and duration of signalling. Several scaffold proteins involved in mammalian JNK signalling modules have been identified, including JIP (JNK-interacting protein) 1, JIP2, JSAP1 [JNK/SAPK (stress-activated protein kinase)-associated protein 1]/JIP3, JLP (JNK-associated leucine-zipper protein) and POSH [plenty of SH3s (Src homology 3)] and their various splice variants. JIP1, JIP2 and JSAP1 bind to JNK, MKK7 and various MLKs. JSAP1 associates with JNK, MKK4 and MEKK1, whereas JLP links Max with c-Myc, and JNK with p38, MKK4 or MEKK3. In addition, multiple upstream MAPKKKs can act as scaffold proteins, as well as exert their intrinsic kinase activities. For example, MEKK1 binds to and regulates MKK4. Despite this flexibility, theoretical considerations have dictated that a single JIP-based MAPK module containing MKK4 and MKK7 physically cannot catalyse the sequential phosphorylation of JNK by these kinases [11]. We therefore speculated that additional scaffold molecules must exist that can bind to and connect two sets of complexes, one containing MKK4 and the other containing MKK7. To identify these presumed 'binder' molecules, we used MKK7 and the yeast two-hybrid method to screen a human leucocyte cDNA library. We isolated Filamin A, which has been previously reported to interact with MKK4 [12], as a predicted 'binder' protein that can also interact with MKK7. Our results show that different MKK7 splice isoforms [13] have different scaffold-binding properties, and that Filamin A plays an important role in synergistic JNK activation.

EXPERIMENTAL

Cell culture

HEK (human embryonic kidney)-293T cells, HeLa cells and non-transfected (M2) or stably transfected (A7) human melanoma cell lines were maintained in DMEM (Dulbecco's modified Eagle's medium) supplemented with 10 % FCS (fetal calf serum), 0.16 % $NaHCO_3$ and 0.6 mg · ml^{-1} L-glutamine. To maintain Filamin A expression, A7 cells were cultured in the presence of 0.5 mg/ml G418 (Sigma).

Antibodies and GFP (green fluorescent protein) vector

Abs (antibodies) against human Filamin A (MAB1680) were from Chemicon. Abs against SAPK/JNK1 (C-17 and FL) or phospho-SAPK/JNK (#9251) were from Santa Cruz Biotechnology and Cell Signaling Technology respectively. Anti-FLAG (M2) and anti-c-Myc (9E10) Abs were from Sigma–Aldrich. Anti-HA (haemagglutinin) high-affinity (3F10) Ab was from Roche Diagnostics. The rat anti-MKK7 (KN-004) mAb (monoclonal Ab) used for immunoprecipitation and immunoblotting was prepared in our laboratory as previously described [7]. Abs against MKK4 (sc-837) or phospho-MKK4 (#9151) were from Santa Cruz Biotechnology and Cell Signaling Technology respectively. The pEGFP-C1 vector was from BD Biosciences.

Construction of plasmids

cDNAs encoding FLAG-tagged versions of MKK4, MKK7α1, MKK7β1, MKK7γ1, MKK7γ2, JNK1 and full-length Filamin A were cloned into the mammalian expression vector pCMV5. Plasmids expressing Myc-tagged full-length Filamin A, the Myc-tagged CT (C-terminus) of Filamin A (residues 2282–2647), or Myc–Filamin B, Myc–Filamin C or HA-tagged MKK4 were also cloned into pCMV5. Myc-tagged Filamin A deletion mutants A, B and C were generated using PCR and subcloned into pCMV5. FLAG-tagged MKK7 deletion mutants A, B and C were constructed using a One Day Mutagenesis kit (QuikChange® kit from Stratagene) and cloned into pCMV5.

Transfection

For gene expression analysis, HEK-293T cells were plated at 6×10^6 cells in a 100-mm dish, or at 2×10^6 cells in a 60-mm dish. Cells were transfected 1 day later with 5 μg (100-mm dish) or 1.8 μg (60-mm dish) of plasmid DNA using 5 μl of Lipofectamine™ 2000 (Invitrogen). M2 cells were plated at 1.25×10^6 cells in a 60-mm dish and transfected 1 day later with 2.5 μg of plasmid DNA as above. After 48 h in culture, cell extracts were prepared and subjected to immunoprecipitation as described below.

Immunoprecipitation and immunoblotting

Transfected HEK-293T cells were resuspended in lysis buffer A [20 mM Hepes/KOH (pH 7.4), 40 mM NaCl, 1 % Triton X-100, 1 mM dithiothreitol, 1 mM EDTA, 2 mM EGTA and 0.1 mM PMSF] at 4 °C. Cell lysates were incubated with anti-FLAG M2 agarose (Sigma) at 4 °C for 2 h. The immunocomplexes were washed several times with lysis buffer A and eluted with 200 μg/ml FLAG peptides. The eluted samples were fractionated by SDS/PAGE and proteins were electrophoretically transferred on to a PVDF membrane (Bio-Rad). Membranes were immunoblotted with anti-FLAG, anti-Myc, anti-HA or anti-(Filamin A) Abs. Bands were visualized using SuperSignal West Pico Chemiluminescent Substrate for the development of immunoblots and a HRP (horseradish peroxidase)-conjugated secondary Ab, according to the manufacturer's instructions (Pierce).

Assay of JNK and MKK7 activities

Confluent melanoma cells were treated at 37 °C for 20 min with sorbitol (50, 100, 150, 200, 300 or 500 mM). Treated cells were washed and resuspended in lysis buffer B [100 mM NaCl, 40 mM Tris/HCl (pH 8.0), 1 % Nonidet P40, 0.05 % 2-mercaptoethanol, 1 mM EDTA, 1 mM EGTA and 4 μg/ml aprotinin]. Extracts were incubated for 2 h at 4 °C with anti-JNK pAb (polyclonal antibody; C-17, Santa Cruz Biotechnology) to immunoprecipitate JNK proteins. Endogenous MKK7 proteins were immunoprecipitated in a similar manner with anti-MKK7 (KN-004) mAb. Immunocomplexes were washed three times with lysis buffer B and three times with kinase reaction buffer [10 mM $MgCl_2$, 50 mM Tris/HCl (pH 7.5) and 1 mM EGTA]. JNK activity in immunoprecipitates was measured using a previously described *in vitro* kinase assay [6,7] employing 60 μM [γ-^{32}P]ATP and GST (glutathione transferase)–c-Jun as the substrate. MKK7 activity on beads was measured using an *in vitro* MAPK kinase assay [6,7] employing 100 μM unlabelled ATP with GST–JNK1 as the substrate; the product was detected using an anti-phospho-JNK Ab. For both *in vitro* kinase assays, the reactions were terminated after 30 min at 30 °C by the addition of 10 μl of 4×SDS gel sample buffer.

To assay JNK activity in transfected M2 cells, cells were resuspended in lysis buffer C [150 mM NaCl, 40 mM Hepes (pH 7.4), 1 % Nonidet P40, 0.05 % 2-mercaptoethanol, 1 mM EDTA, 1 mM EGTA, 10 mM $MgCl_2$ and 4 μg/ml aprotinin]. The resulting cell lysates were analysed by SDS/PAGE and immunoblotting in which JNK activation was detected using an anti-phospho-JNK Ab.

Yeast two-hybrid assay

A human brain cDNA library (Clontech) and the MatchMaker™ GAL4 Two-Hybrid System 3 (Clontech) were used, as described previously [14], for a yeast two-hybrid assay in which MKK7 served as the bait.

Confocal microscopy

HeLa cells transiently expressing GFP–MKK7γ1 were cultured on a polylysine-coated glass coverslip (15-mm diameter) and washed three times with PBS before fixation with 4 % (w/v) paraformaldehyde in PBS for 15 min at 4 °C. After treatment with 0.1 mM glycine in PBS for 15 min, the cells were permeabilized with 0.1 % Triton X-100 in blocking solution (3 % BSA in PBS) before incubation for 1 h at room temperature (25 °C) with rhodamine-conjugated phalloidin diluted in blocking solution. After three PBS washes, the coverslip was mounted on to a glass slide in Permafluor-mounting medium (Immunon) and viewed using a confocal microscope (Carl Zeiss) with LSM510 software. Excitation wavelengths of 488 nm or 546 nm were used. The images were merged using Photoshop (Adobe Systems).

For overexpression of GFP-tagged Filamin A, GFP–MKK7α1, GFP–MKK7γ1 or GFP–MKK7 deletion B, and for co-expression of GFP-tagged MKK7γ1 and a fusion protein composed of red fluorescent protein (DsRed) plus Filamin A, transfected HeLa cells were cultured for 48 h in a glass-based dish (35-mm diameter; Iwaki) and examined by confocal microscopy as described previously [14].

RESULTS

Interaction of Filamin A with MKK4 and MKK7

To identify proteins that interacted with both MKK4 and MKK7, a human leucocyte cDNA library was screened with MKK7 in a yeast two-hybrid system. Among various MKK7-binding cDNAs isolated were several encoding the CT of ABP-280 (actin-binding protein-280, Filamin A), which was previously reported to bind to MKK4 [12]. To determine whether endogenous full-length Filamin A could interact with both MKK4 and MKK7 *in vivo*, we transiently overexpressed FLAG–MKK4, FLAG–MKK7γ2 and FLAG–JNK1 in HEK-293T cells and carried out co-immunoprecipitation experiments. As shown in Figure 1(A), a protein of ~280 kDa co-immunoprecipitated with FLAG–MKK4 and FLAG–MKK7γ2, but not with FLAG–JNK1. We confirmed that this 280 kDa protein was indeed Filamin A using Western blotting employing anti-(Filamin A) Ab (Figure 1B). We next used FLAG and Myc tagging to examine whether two other members of the Filamin protein family, Filamin B and Filamin C, could bind to MKK4 and MKK7 *in vivo*. When overexpressed in HEK-293T cells, both Filamin B and Filamin C co-immunoprecipitated with both MKK4 and MKK7γ2 (Figure 1C). These results show that Filamin family proteins can interact with at least two MAPKKs, MKK4 and MKK7γ2, and demonstrate a novel connection between an MKK7 enzyme and a Filamin protein known to interact with MKK4.

Isoform-specific interaction of MKK7 with Filamin A

To date, six isoforms of MKK7 have been identified [12]. To test whether four of these MKK7 isoforms (Figure 2A) interacted differentially with Filamin A, HEK-293T cells were transiently co-transfected with individual FLAG–MKK7 isoforms plus Myc-tagged Filamin A (CT). As shown in Figure 2(B), Myc–Filamin A (CT) co-immunoprecipitated with FLAG–MKK7γ2, FLAG–MKK7γ1 and FLAG–MKK7β1, but not with FLAG–MKK7α1. We next constructed three deletion mutants of MKK7γ1 (MKK7γ1 deletion A, B and C; Figure 2A) that affected the presumed Filamin-A-binding site in MKK7 and repeated the co-immunoprecipitation experiments. Myc–Filamin A (CT) co-immunoprecipitated with FLAG–MKK7γ1 deletion A and deletion C, but not with FLAG–MKK7γ1 deletion B or FLAG–MKK7α1 (Figure 2C). Thus a short N-terminal region (encompassing amino acids 31–60) that is present in MKK7γ and MKK7β, but absent in MKK7α1, is required for MKK7 binding to Filamin A.

Co-localization of MKK7 with Filamin A

To investigate whether MKK7 co-localizes with Filamin A in cells, we first examined the subcellular localization of MKK7γ1 and found that this isoform associated with fibre-like structures. To determine whether these fibres were actin stress fibres, HeLa cells were transiently transfected with GFP-tagged MKK7γ1, fixed, stained with phalloidin to visualize actin distribution, and examined by confocal microscopy. We observed that MKK7γ1 did indeed co-localize with actin stress fibres (Figure 3A). Because Filamin A is known to cross-link actin filaments, these results suggested that MKK7γ1 co-localized with Filamin A. We tested this possibility by transfecting HeLa cells with GFP–MKK7γ1 and DsRed–Filamin A. As expected, MKK7γ1 co-localized with Filamin A in selected areas (Figure 3B). To investigate whether the apparent association of MKK7γ1 with actin stress fibres was due to the interaction of MKK7γ1 with Filamin A, HeLa cells were co-transfected with GFP–Filamin A and GFP–MKK7γ1, GFP–MKK7γ1 deletion B or GFP–phospho-MKK7α1. Confocal microscopy showed that GFP–MKK7γ1 and GFP–Filamin A co-localized on fibre-like structures, whereas GFP–MKK7α1 and GFP–MKK7γ1 deletion B (which do not interact with Filamin A) were diffusely distributed throughout the cytoplasm (Figure 3C). Thus MKK7γ1 and Filamin A co-localize in cells, and MKK7γ1 associates with actin stress fibres due to its interaction with Filamin A.

Filamin A mediates a connection between MKK4 and MKK7γ

The above experiments showed that Filamin A interacts not only with MKK4, but also with MKK7γ and MKKβ isoforms. To identify the regions of Filamin A that can interact with MKK4 or MKK7γ, HEK-293T cells were transiently co-transfected with either Myc–Filamin A (CT), including its MKK4-binding region (amino acids 2282–2454), or a series of Filamin A deletion mutant proteins lacking different portions of the MKK4-binding region (Figure 4A), together with FLAG–MKK4 or FLAG–MKK7γ2. Co-immunoprecipitation assays showed that amino acids 2297–2311 of Filamin A were required for its interaction with MKK7γ2 (Figure 4B). Thus the region of Filamin A required for binding to MKK7γ2 is distinct from that needed for the interaction with MKK4. We then investigated whether Filamin A could interact simultaneously with MKK4 and MKK7γ2 by transiently co-transfecting HEK-293T cells with HA-tagged MKK4 plus FLAG–MKK7γ2 or FLAG–MKK7α1. HA–MKK4

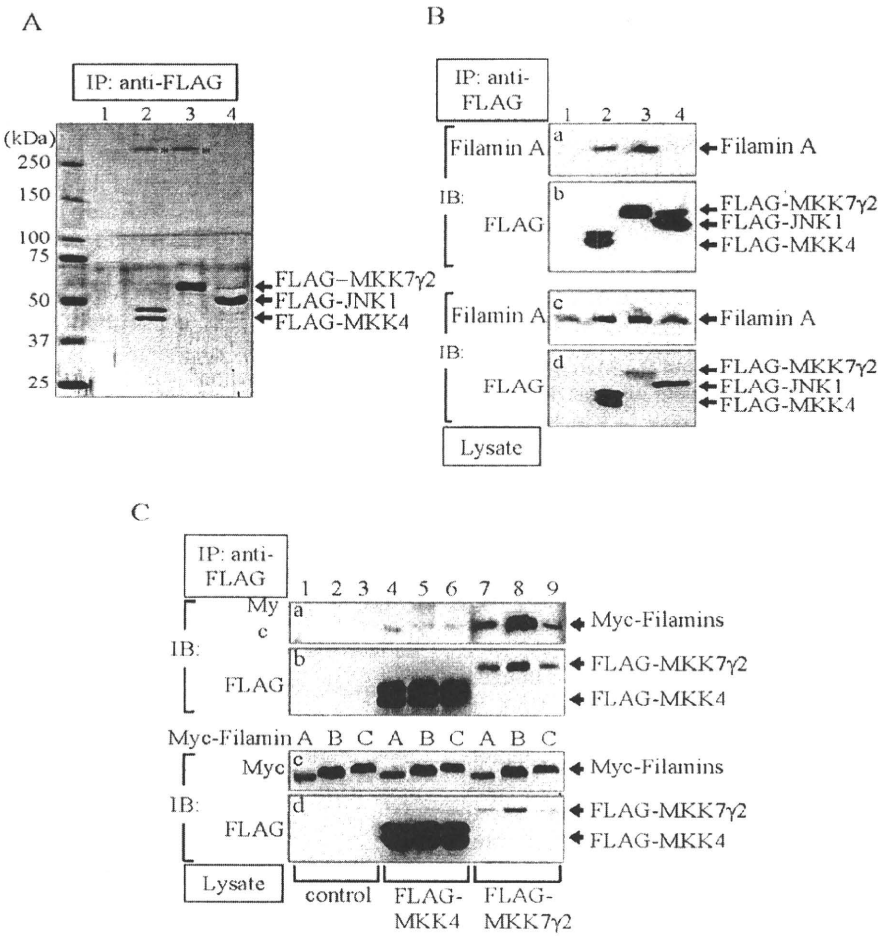

Figure 1 Interaction of Filamin A with MKK4 and MKK7

(**A** and **B**) HEK-293T cells were transfected with 5 μg of pCMV5/FLAG (lanes 1), FLAG–MKK4 (lanes 2), FLAG–MKK7γ2 (lanes 3) or FLAG–JNK1 (lanes 4). Cell lysates were prepared (**B**, panels c and d) and immunoprecipitated (IP) with anti-FLAG M2 agarose (**A** and **B**, panels a and b). (**A**) Co-immunoprecipitated proteins (*) were visualized using Coomassie Blue. The molecular mass in kDa is indicated on the left-hand side. (**B**) Co-immunoprecipitated Filamin A and immunoprecipitated FLAG–MKK4, FLAG–MKK7γ2 and FLAG–JNK1 were identified using anti-(Filamin A) (panel a) and anti-FLAG M2 (panel b) Abs respectively. Expression of Filamin A and FLAG–MKK4, FLAG–MKK7γ2 and FLAG–JNK1 were determined by immunoblotting (IB) using anti-(Filamin A) (panel c) and anti-FLAG M2 (panel d) Abs respectively. (**C**) HEK-293T cells were transfected with 0.9 μg of pCMV5/Myc-Filamin A (CT) (lanes 1, 4 and 7), Myc–Filamin B (lanes 2, 5 and 8) or Myc–Filamin C (lanes 3, 6 and 9), together with 0.9 μg of pCMV5/FLAG (lanes 1–3), FLAG–MKK4 (lanes 4–6) or FLAG–MKK7γ2 (lanes 7–9). Cell lysates were prepared (panels c and d) and immunoprecipitated (IP) with anti-FLAG M2 agarose (panels a and b). Co-immunoprecipitated Myc–Filamin proteins and immunoprecipitated FLAG–MKK4 and FLAG–MKK7γ2 were determined using anti-c-Myc (panel a) and anti-FLAG M2 (panel b) Abs respectively. Expression of Myc–Filamin proteins and FLAG–MKK4 and FLAG–MKK7γ2 were determined using anti-c-Myc (panel c) and anti-FLAG M2 (panel d) Abs respectively. IB, immunoblot.

and endogenous Filamin A co-immunoprecipitated with FLAG–MKK7γ2, but not with FLAG–MKK7α1 (Figure 4C). Because this experiment did not exclude the possibility that MKK4 might interact directly with MKK7γ2 (rather than with Filamin A), we repeated these co-immunoprecipitation experiments using a human melanoma cell line M2 that has spontaneously lost expression of Filamin A [15]. M2 cells were transiently co-transfected with HA–MKK4 and FLAG–MKK7γ2, together with increasing amounts of Myc–Filamin A (CT). Interaction of MKK4 with MKK7 was enhanced when higher amounts of Filamin A (CT) were present (Figure 4D), suggesting that Filamin A, MKK4 and MKK7γ2 form a complex in which Filamin A connects MKK4 and MKK7γ2.

Filamin A enhances the activation of MKK7 and JNK

The above results suggested that Filamin A might be one of the 'binder' proteins predicted to closely connect two MAPKKs within a MAPK module in living cells [11]. To examine the effect of Filamin A on JNK activation *in vivo*, we compared JNK activation in M2 cells (no Filamin A expression) with that in A7 cells (M2 cells stably transfected with a vector expressing full-length human Filamin A; [16]). In response to increasing concentrations of sorbitol, JNK was activated much more strongly in A7 cells than in M2 cells (Figure 5A). When we analysed the activation state of MKK7 in these sorbitol-treated M2 and A7 cells, we found that 500 mM sorbitol induced a 3.3-fold activation of MKK7 in A7 cells, but only a 1.4-fold activation of MKK7 in M2 cells (Figure 5B). The activation of MKK4 is also higher in A7 cells than in M2 cells (Figure 5C). Thus, in living cells, Filamin A promotes optimal stress-induced JNK activation by enhancing MKK7 and MKK4 activation.

Finally, we analysed the effect of Filamin A on JNK activation induced by overexpression of MKK4 and/or MKK7γ2. M2 cells were transiently transfected with FLAG–MKK4 and FLAG–MKK7γ2, together with various amounts of FLAG–Filamin A. Overexpression of MKK7γ2 and MKK4 induced JNK activation which was greatly enhanced when the amount of transfected

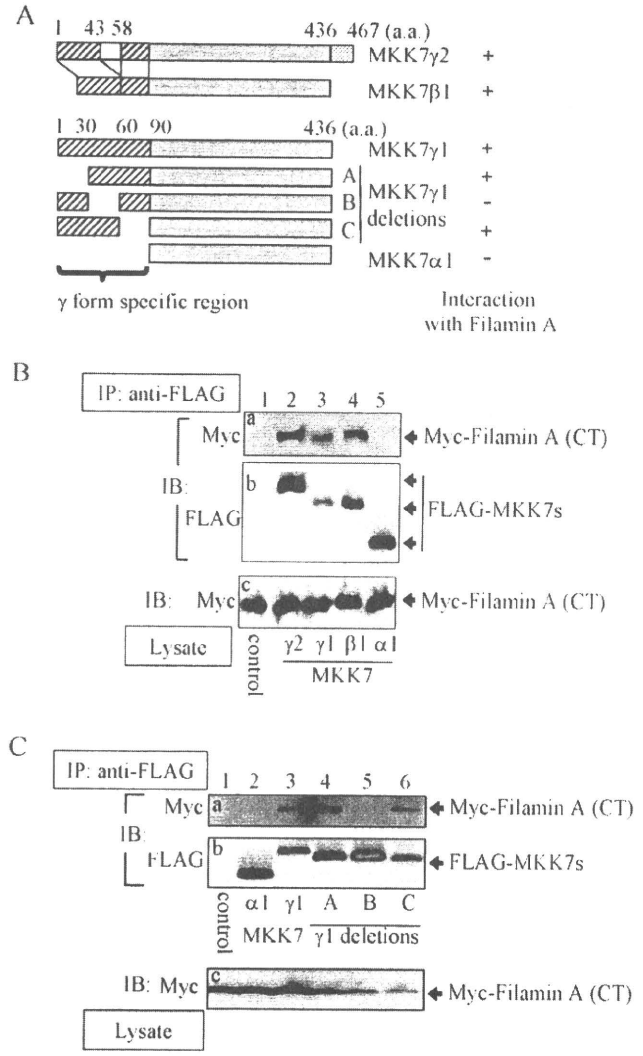

Figure 2 Isoform-specific interaction of MKK7 with Filamin A

(**A**) Schematic diagram of MKK7 isoforms and deletion mutants (A, B and C). The ability of each protein to interact with Filamin A is indicated. a.a., amino acid. (**B**) HEK-293T cells were co-transfected with 0.9 μg of pCMV5/FLAG (lane 1), or FLAG–MKK7 isoforms γ2 (lane 2), γ1 (lane 3), β1 (lane 4) or α1 (lane 5), together with 0.9 μg of pCMV5/Myc-Filamin A (CT). (**C**) HEK-293T cells were transfected with 0.9 μg of pCMV5/FLAG (lane 1), or FLAG–MKK7 isoforms α1 (lane 2), γ1 (lane 3), γ1 deletion A (lane 4), γ1 deletion B (lane 5) or γ1 deletion C (lane 6), together with 0.9 μg of pCMV5/Myc-Filamin A (CT). Co-immunoprecipitated Myc–Filamin A (CT) and immunoprecipitated FLAG–MKK7s were identified using anti-c-Myc (panel a) and anti-FLAG M2 (panel b) Abs respectively. Expression of Myc–Filamin A (CT) was determined using anti-c-Myc (panel c). IB, immunoblot; IP, immunoprecipitation.

Filamin A was increased (Figure 5D, upper panel). However, MKK4- or MKK7γ2-induced JNK activation was not enhanced when the amount of transfected Filamin A was increased (Figure 5D, lower panel). These results support our contention that, by physically connecting MKK4 and MKK7γ2, Filamin A facilitates synergistic JNK activation dependent on these MAPKKs.

DISCUSSION

In vitro experiments have shown that synergistic activation of JNK requires the phosphorylation of both the threonine and tyrosine residues within the threonine-proline-tyrosine motif of JNK, and that this phosphorylation is mediated by two different enzymes, MKK4 (SEK1) and MKK7 [3–5]. Although both of

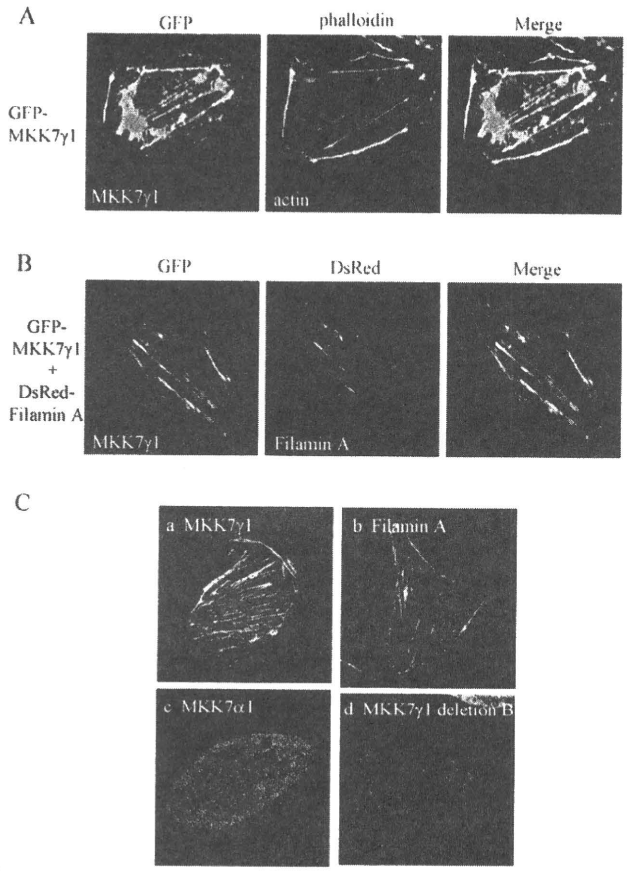

Figure 3 Co-localization of MKK7γ isoforms with Filamin A

(**A**) HeLa cells were transiently transfected with 1.2 μg of GFP–MKK7γ1 and cultured for 48 h. Actin was identified by rhodamine–phalloidin staining, and individual and merged images (yellow) were visualized using confocal scanning microscopy. (**B**) HeLa cells were transiently co-transfected with 0.6 μg of GFP–MKK7γ1 plus 0.6 μg of DsRed–Filamin A. Images were visualized as for (**A**). (**C**) HeLa cells were transiently transfected with 1.2 μg of GFP–MKK7γ1 (panel a), GFP–Filamin A (panel b), GFP–MKK7α1 (panel c) or GFP–MKK7γ1 deletion B (panel d), and cultured for 48 h prior to examination by confocal microscopy.

these MAPKKs can catalyse the phosphorylation of both tyrosine and threonine, MKK4 preferentially phosphorylates the tyrosine residue, whereas MKK7 preferentially phosphorylates the threonine residue [3]. In a previous study of stress-stimulated murine ES cells, we presented *in vivo* data confirming that these key tyrosine and threonine residues of JNK are sequentially phosphorylated by MKK4 and MKK7 respectively [7,11] (Figure 6A). The present study provides evidence that Filamin A is one of the 'binder' molecules presumed to directly and closely connect MKK4 and MKK7 so that they can mediate this tyrosine/threonine phosphorylation. We showed that Filamin A (as well as Filamin B and C) associate with MKK7 and MKK4, but not with JNK1 itself (Figure 1). Furthermore, this association is isoform-specific, since Filamin A interacted with MKK7γ and MKK7β, but not with MKK7α (Figure 2). In addition, MKK7γ (but not MKK7α) co-localized with actin filaments in a manner dependent on Filamin A binding (Figure 3). We also showed that the MKK7-binding site of Filamin A was different from that for MKK4, and that the formation of the MKK7γ–MKK4 complex was mediated by Filamin A (Figure 4). Lastly, we demonstrated that Filamin A was essential for strong JNK, MKK7 and MKK4 activation in response to sorbitol, as well as for induction of JNK activation by MKK4 and MKK7

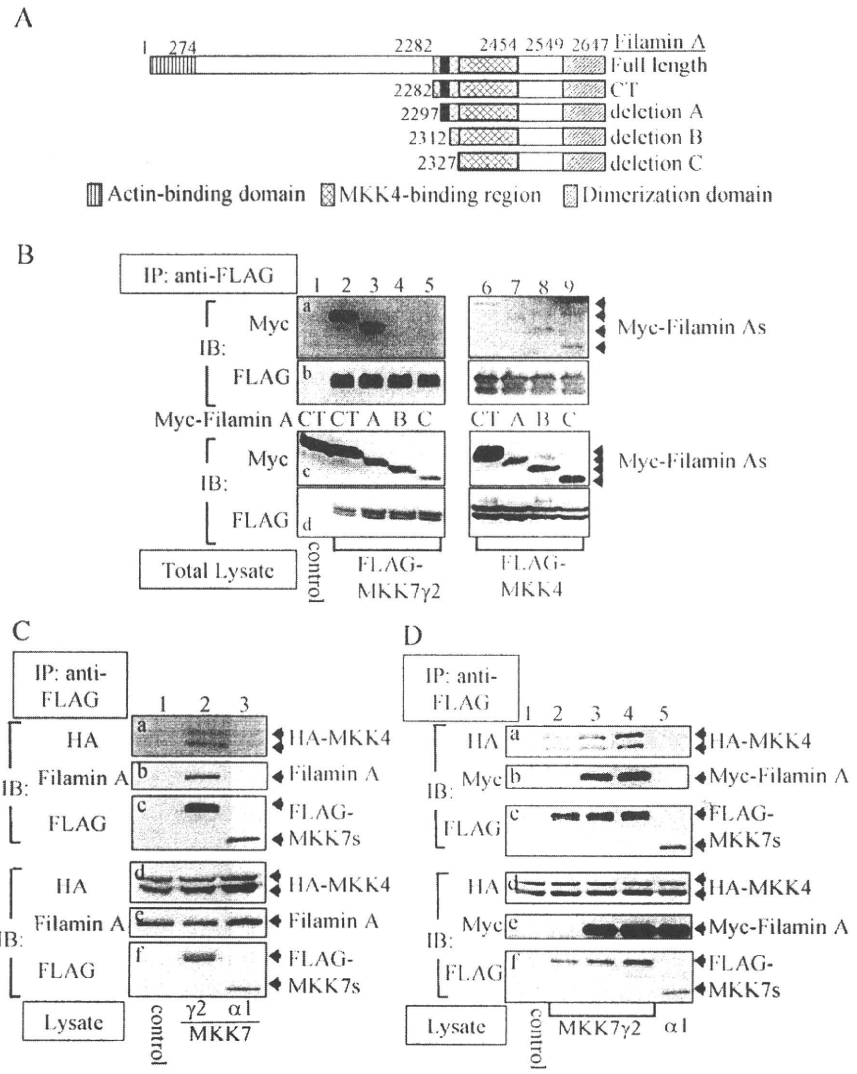

Figure 4 Filamin-A-mediated connection of MKK4 and MKK7γ

(**A** and **B**) Deletion analysis identifying the MKK7-binding region of Filamin A. (**A**) Schematic diagram of Filamin A proteins, including full-length, CT and deletion mutants A, B and C. Relevant domains are indicated. (**B**) HEK-293T cells were co-transfected with 0.9 μg of pCMV5/Myc-Filamin A (CT) (lanes 1, 2, and 6), or Myc–Filamin A deletion A (lanes 3 and 7), Myc–Filamin A deletion B (lanes 4 and 8) or Myc–Filamin A deletion C (lanes 5 and 9), together with 0.9 μg of pCMV5/FLAG (lane 1), FLAG–MKK7γ2 (lanes 2–5) or FLAG–MKK4 (lanes 6–9). Co-immunoprecipitated Myc–Filamin A proteins and immunoprecipitated FLAG–MKK7γ2 or FLAG–MKK4 were identified using anti-c-Myc (panel a) and anti-FLAG M2 (panel b) Abs respectively. Expression of Myc–Filamin A proteins and FLAG–MKK7γ2 or FLAG–MKK4 were determined using anti-c-Myc (panel c) and anti-FLAG M2 (panel d) Abs respectively. (**C**) HEK-293T cells were transfected with 2 μg of pCMV5/HA-tagged MKK4, together with 3 μg of pCMV5/FLAG (lane 1), pCMV5/FLAG-MKK7γ2 (lane 2) or pCMV5/FLAG-MKK7α1 (lane 3). Co-immunoprecipitated HA–MKK4, endogenous Filamin A and immunoprecipitated FLAG–MKK7 were determined using anti-HA (panel a), anti-Filamin A (panel b) and anti-FLAG M2 (panel c) Abs respectively. Expression levels of HA–MKK4, endogenous Filamin A and FLAG–MKK7 proteins were determined using anti-HA (panel d), anti-Filamin A (panel e) and anti-FLAG M2 (panel f) Abs respectively. (**D**) M2 human melanoma cells were co-transfected with various amounts of pCMV5/Myc-Filamin A (CT) (0, 0, 1, 2 and 2 μg in lanes 1–5 respectively), plus 3 μg of pCMV5/FLAG (lane 1), pCMV5/FLAG-MKK7γ2 (lanes 2–4) or pCMV5/FLAG-MKK7α1 (lane 5), together with 2 μg of pCMV5/HA-tagged MKK4. Co-immunoprecipitated HA–MKK4, Myc–Filamin A (CT) and immunoprecipitated FLAG–MKK7 proteins were determined using anti-HA (panel a), anti-c-Myc (panel b) and anti-FLAG M2 (panel c) Abs respectively. Expression of HA–MKK4, Myc–Filamin A and FLAG–MKK7 proteins was determined using anti-HA (panel d), anti-c-Myc (panel e) and anti-FLAG M2 (panel f) Abs respectively. IB, immunoblot; IP, immunoprecipitation.

(Figure 5). Thus we present a novel model in which MKK4 and MKK7γ use Filamin A as a scaffold to support their sequential tyrosine/threonine phosphorylation and thus synergistic activation of JNK (Figure 6B).

Our work clarifies that there are at least three types of JNK activation mechanisms: (i) MKK4-mediated JNK phosphorylation, (ii) MKK7-mediated JNK phosphorylation, and (iii) JNK phosphorylation mediated by both MKK4 and MKK7. Molecular mechanisms (i) and (ii) depend on the JNK scaffold proteins JIP1, JIP2, JSAP1 and JLP, which bind to JNK and MKK4 or MKK7, but not to all three proteins [10]. In contrast, mechanism (iii) depends on a Filamin protein (A, B or C), rather than on a JIP-type protein. We speculate that, in living cells, there may be a wide variety of JNK activation and signalling modules that involve either JIP-type or Filamin-type molecules, or a combination of these scaffold proteins depending on different cell types. The ratios of the JNK signalling modules seem to vary in different cell types.

Filamin A is an actin cross-linking protein and possesses an actin-binding domain and a homodimerization domain that allow it to determine the submembranous cytoskeletal architecture of cells. Consistent with these properties, Filamin A is required for cell adhesion and migration [15]. Previous studies have shown that Filamin A interacts with MKK4 and TRAF2 [TNF